1-1-2016

PKA-Rap1A Dependent Regulation of Age-Rage Signaling in Type II Diabetes Mellitus

Rebecca Anne Worsham

PKA-Rap1a dependent regulation of AGE-RAGE signaling in type II diabetes mellitus

By

Rebecca Anne Worsham

A Thesis
Submitted to the Faculty of
Mississippi State University
in Partial Fulfillment of the Requirements
for the Degree of Master of Science
in Biological Sciences
in the Department of Biological Sciences

Mississippi State, Mississippi

May 2016

PKA-Rap1a dependent regulation of AGE-RAGE signaling in type II diabetes mellitus

By

Rebecca Anne Worsham

Approved:

_____

James A. Stewart, Jr.
(Major Professor)

_____

Donna M. Gordon
(Committee Member)

_____

Florencia Meyer
(Committee Member)

_____

Mark E. Welch
(Graduate Coordinator)

_____

Rick Travis
Interim Dean
College of Arts & Sciences

Name: Rebecca Anne Worsham

Date of Degree: May 6, 2016

Institution: Mississippi State University

Major Field: Biological Sciences

Major Professor: James A. Stewart, Jr.

Title of Study: PKA-Rap1a dependent regulation of AGE-RAGE signaling in type II diabetes mellitus

Pages in Study: 80

Candidate for Degree of Master of Science

Type II diabetes mellitus is associated with many detrimental health situations including heart complications. The purpose of this study was to identify a role for PKA-dependent Rap1a signaling in the AGE-RAGE cascade. My hypothesis was Rap1a GTPase increased the downstream effects of AGE-RAGE signaling in diabetes via a PKA-dependent pathway leading to elevated ECM remodeling in the heart. Cardiac fibroblasts were isolated from heterozygous (Het) and diabetic (db/db) mice. To test the hypothesis, gain-of-function and loss-of-function treatments were used. PKC-Zeta is known as a major signaling hub that potentially links PKA-dependent and AGE-RAGE signaling cascades so PKC-Zeta inhibition to downregulate PKA-dependent cascade at PKC-Zeta was also used. Results showed a downregulation of signaling markers in the AGE-RAGE cascade when disrupting Rap1a crosstalk at PKC-Zeta. By understanding where the PKA-dependent and AGE-RAGE signaling cascades crosstalk, a new molecular mechanism is understood possibly leading to decreasing remodeling in a diabetic heart.

ACKNOWLEDGEMENTS

To begin, I would like to acknowledge my major professor, James A. Stewart, Jr., Ph.D., for having the patience and giving me endless support and guidance throughout my graduate school career. I definitely would not have survived without you being my major professor! I also would like to acknowledge all of my lab co-workers including Carter Holland, Neeta Kumari, and Jessie Zhao for helping me learn new techniques and answering any of my questions. I am very grateful for the undergraduates who helped me with my project including Rosalynn Gunn, Caroline Lightsey, and Sasha Shurden. Sasha, words cannot even begin to describe how thankful I was to have you by my side to keep my research going with your endless gel making so THANK YOU!! A big hug goes to Ashley Reeves and Jessica Dougan for keeping my sanity and stress at a somewhat normal level throughout these years of graduate school. Thank you Mo Eguires and Amy Richardson for doing all what y'all did for me and pushing me during the final stages of completing my thesis! I also want to thank my Mom, Dad, Sister, and Mamaw for supporting me throughout my undergraduate and graduate years. (But I am not quite done yet…medical school is in the future!!). Last, but not least, I want to thank Mississippi State University, specifically the Stewart lab in the Department of Biological Sciences for providing me an opportunity to further my education with a master's degree as well as knowledge obtained regarding health-related research that will aid in becoming a physician in the future.

TABLE OF CONTENTS

LIST OF FIGURES

CHAPTER I

LITERATURE REVIEW

Introduction

According to the American Diabetes Association (ADA), diabetes mellitus is defined as a family of diseases characterized by high blood glucose levels (hyperglycemia) resulting from the body's inability to produce and/or use the hormone insulin[3]. β Cells, found in clusters or islets, in the pancreas, are responsible for the production of insulin and its release into the blood[47]. There are three types of diabetes mellitus: type I, type II, and gestational or type III.

Type I diabetes, which occurs when the β cells of the pancreas do not produce sufficient levels of insulin, resulting in administration of daily injections of insulin to maintain normoglycemic levels in the body. Type 1 diabetes mellitus can occur at any age; however, it frequently diagnosed in children, teens, or young adults. Type II diabetes is the more common type of diabetes occurring most often in adults; however, diagnosis of type II diabetes in teens and young adults is becoming more prominent due to increasing obesity rates[47]. Type II diabetes results from insulin resistance, which is a condition whereby the body's fat, muscle, and liver cells do not use insulin effectively. The body attempts to compensate for the impaired ability to use insulin by increasing the amount of insulin produced, resulting in hyperinsulinemia. Hyperinsulinemia results in a desensitization of the insulin receptor[40]. When the body is no longer able to respond to

insulin levels, type II diabetes develops[47]. Gestational diabetes or type III diabetes mellitus, as the name implies, is characterized by high blood sugar levels during any point of pregnancy in a woman who has not been diagnosed with diabetes prior to pregnancy[47]. In addition to the three types of diabetes mellitus, prediabetes or borderline diabetes has been recognized as a risk factor for the development of type II diabetes. As a precursor or early diabetes stage, prediabetes is considered a "grey area" whereby fasting blood glucose levels are higher than normal (100 – 125 mg/dL) but not quite high enough to diagnose as diabetes (>126 mg/dL)[47]. Thus, patients with pre-diabetes have an increased risk of developing heart disease, type II diabetes, and having a stroke are significantly higher[48]. According to the 2014 National Diabetes Statistics Report, 86 million Americans aged 20 and older have pre-diabetes and 29.1 million Americans, or 9.3% of the U.S. population, have diabetes[15]. Diabetes was the seventh leading cause of death in the U.S. in 2010, and risk of death in adults with diabetes is 50% higher than without diabetes[15].

Chronic hyperglycemia can lead to many long-term complications in multiple organ systems. In particular, there is a strong correlation between diabetes and cardiovascular disease[31,82]. The 2014 National Diabetes Statistics Report showed hospitalization rates in 2010 for heart attack and stroke, after adjusting for population age differences, were 1.8 and 1.5 times higher, respectively, among adults aged 20 years and older with diagnosed diabetes as compared to adults without diagnosed diabetes[15]. One complication found in the cardiovascular system, resulting from diabetes, is increased extracellular matrix (ECM) accumulation[31,82]. Increased ECM accumulation, also referred

to as interstitial fibrosis, occurs when there is an increase in crosslinks between glucose and the structural protein collagen, which decreases proper heart function[31,82].

Extracellular Matrix

Extracellular matrix (ECM) is made up of macromolecular proteoglycans, proteases, collagens, glycoproteins, growth factors, and cytokines[11,82]. The ECM plays a role in communication between cells and collaborative organ-level functions, provides structural support, and is critical in maintaining homeostasis and pathological remodeling[11,82]. The ECM facilitates mechanical, electrical, and chemical signals not only during the developmental process and homeostasis, to induce cell proliferation, migration, and adhesion, but also in response to physiological stress or injury in cardiac physiology to mediate changes in gene expression[7,11,82].

Collagen

A necessary component of the ECM is fibrillar collagen. Collagen is one of the most abundant proteins in the body[11,26,82]. The fibrillar collagen superfamily is composed of 28 different collagen types. The criteria that distinguish members of this superfamily are often not well defined; however, one feature that is common among this family is a triple helix structure[11,26,82]. The triple helical component of collagen can range from >96% as found in collagen I to <10% as seen in collagen XII[56]. The diversity of collagens has been attributed to a number of factors, such as the presence of several alpha (α) chains, multiple molecular isoforms for single collagen types, as well as the presence of alternative promoters and splice variants[26,56]. Of these various factors, α chains contribute to the highest degree of structural diversity[56]. Collagen α chain can vary in size. For

example, the α1 chain of collagen X has ~662 amino acids, whereas the α3 chain of collagen VI has ~3125 amino acids[25,57]. Additionally, the α amino acid sequence, number of glycine, proline, and hydroxyproline repeats, formation of either homo- or heterotrimers, and left- or right hand directional twists contribute to the variations observed in the collagen superfamily[56]. For example, alternative transcriptional start sites, but with the same transcriptional factor, will generate different forms of the α1 for collagen IX and XVIII chains. Alternative gene splicing will contribute to the formation of several isoforms of the following collagen chains: α1 collagen II, α2 collagen VI, α3 collagen VI, α1 collagen VII, α1 collagen XII, α1 collagen XIII, α1 collagen XIV, α1 collagen XIX, α1 collagen XXV, and α1 collagen XXVIII[56,69,73].

The structural variability observed in the collagen superfamily contributes significantly to the functional diversity. For example, the fibrillar nature of the triple helices of collagens I, II, III, and V is rigid due to the presence of glycine, proline, and hydroxyproline repeats; however, the variability and interruptions of these repeats in collagen IV chains results in an increased plasticity and a more flexible type of collagen[41,56]. The structural and functional diversity of the collagen superfamily lends itself to both organ and tissue specificity.

The collagens found in the myocardium include types I, III, IV, V, VI, and VIII with collagen types I and III the most abundant making up 85% and 11%, respectively, in healthy mammalian hearts[26,71]. Synthesis and degradation of the collagens as well as maintenance of collagen ratios are highly coordinated since different types of collagen will convey unique mechanical properties[11,26,71]. Type I collagen influences the overall stiffness of the myocardium due to the combination of extremely high tensile strength

and by forming super-twisted microfibrils that interconnect with the nearby collagen III fibrils. Therefore, collagen expression in the heart is continuously monitored in order to maintain the structural integrity and mechanical stiffness of the heart[11,26,49,50,71].

Regulation of collagen expression is also rigorously monitored during specific stages of cardiac development or remodeling[11,50]. For example, pathologic heart valve structure and dysfunction may be a result of genetic defects in different collagens[11,50]. Various types of collagen, depending on the stiffness and contractility required, are found in different regions in the heart as well[11,50]. Normally, there is a balance of collagen degradation and synthesis to maintain homeostasis in the ECM; however, following injury, degradation and synthesis can become unbalanced, leading to changes in collagen levels and/or ratios to alter the stiffness of the heart[11,26,50]. Collagen-induced decreased contractility, as a response of cardiac injury, is not only caused by an increase in collagen deposition but also with inadequate changes in collagen ratios due to the types of collagen expressed[11,26,50]. Following injury, not only are there changes in collagen deposition as previously mentioned, but also changes in amount of collagen crosslinking[11,26,50]. Increasing the collagen crosslinks can decrease the conductance of electrical signals and bridging of myocytes by cardiac fibroblasts leading to altered cardiac function[11,26,50]. Changes in collagen expression and degradation after injury are oftentimes coupled with changes in circulating chemokines to further alter the chemical and structural components of the cardiac ECM.

Autocrine and paracrine hormones, such as angiotensin II (Ang II), tumor growth factor-β (TGF-β), aldosterone, and angiotensin-converting enzyme (ACE), regulate collagen deposition[11,65,82]. Cardiac fibroblasts increase collagen synthesis and deposition

as a response to particular biochemicals, such as those listed above, and biomechanical signals, such as changes in contractile force[11,26,35]. TGF-β expression and collagen I synthesis is stimulated by secreted Ang II via fibroblasts[11,26,35]. Ang II not only increases the production of cytokines in myocytes but also enhances fibroblast-cytokine sensitivity[11,26]. TGF-β, fibrosis, and collagen deposition can be decreased by ACE inhibitors, improving outcomes by dampening hypertrophy and fibrosis[11]. Possible mechanism of action is through the inhibition of hydrolysis of *N*-acetyl-seryl-aspartyl-lysl-proline (Ac-SDKP) by ACE, which decreases fibroblasts proliferation and collagen synthesis[11]. Galectin-3 expression, an endogenous lectin involved in inflammatory cell recruitment and increased cytokine secretion, fibroblast proliferation, and ventricular dysfunction, has been shown to be reduced by Ac-SDKP[11]. Galectin-3 inhibition results in reduced fibroblast proliferation, collagen deposition, and inhibited macrophage activation and migration[11]. Thus, following Galectin-3 inhibition treatment there is a decrease in cardiac dysfunction[11]. Also, chronic activation of the renin-angiotensin system involves the presence of inflammatory cells and activating fibroblasts to create changes in the cardiovasculature as well as affecting cell recruitment and collagen disposition, leading to a fibrotic state[11].

Fibroblasts

The heart is composed of four major cell types: myocytes, endothelial cells, smooth muscle cells in vessels, and fibroblasts[6,7,64]. Myocytes make 70%-80% of the cellular mass while the remaining 20%-30% includes fibroblasts, vascular smooth muscle cells, and endothelial cells. Fibroblasts being the most abundant of the latter

percentage[7,83]. Fibroblasts are found in many different tissues of the body[6]. In the heart, fibroblasts appear as flattened, elongated cells arranged in sheets and/or strands that lie parallel to the cardiac myocytes connecting them to the endomysial collagen network[6,12]. Fibroblasts are able to respond to electrical, chemical, and biomechanical stimuli in the heart as well as the three-dimensional structure of the organ through autocrine, paracrine, and cell-cell interactions[7,12]. An example is how cardiac myocytes and fibroblasts interact via connexins (Cx40, Cx43, Cx45) in the heart to function in electrical conduction[7,11,64]. However, during cardiac remodeling, these interactions are destroyed leading to interference in the electrical conduction system and thus to pathological conditions[7,35]. Essentially, fibroblasts form the extracellular "glue" responsible for holding the heart together during the duress of cardiac contraction[6,7]. Fibroblasts are considered to be the primary cell type that produces the bulk of the ECM components, such as fibronectin and collagen types I and III[11,82].

Fibroblasts also secrete enzymes such as matrix metalloproteases (MMPs), which promote collagen degradation and turnover of the ECM[35,82]. In addition to MMPs, fibroblasts also secrete periostin as well as various paracrine and autocrine factors including interleukin-6 (IL-6), transforming growth factor-β (TGF-β), endothelin-1 and tumor necrosis factor-α (TNF-α) to promote increased ECM production and/or degradation[11,35,65,82]. In addition, fibroblasts are able to respond to circulating factors, such as angiotensin II and TGF-β, to mediate interactions between fibroblasts and the ECM[35,82].

Cardiac fibroblasts are also sensitive to electrical, chemical, and biomechanical stimulation[7,11]. Force generation, receptor expression and chemical signaling, which are

all important in terms of proper cardiac function, are affected by the ECM composition and organization[7,11]. Therefore, fibroblasts play a vital role in maintaining homeostasis of the ECM[7,11,36]. Once development is complete, many genes are no longer expressed; however, after remodeling, such as after injury (myocardial infarction or MI), these genes are often re-expressed[11,50]. Cardiac fibroblasts, normally, are the primary cells to produce ECM proteins, however, myofibroblasts or activated fibroblasts, neutrophils, mast cells, and macrophages also produce ECM proteins in pathological states such as a MI[11,50].

Myofibroblast

Chronic exposure to pathophysiological conditions, such as hyperglycemia, will cause fibroblasts to become "stressed out" resulting in a phenotypic alteration. Fibroblasts differentiate into myofibroblasts when the cell converts from a normal, inactive quiescent state into an active state[64,68,80]. The conversion of fibroblasts into myofibroblasts is promoted by numerous players including transforming growth factor (TGF-β), cytokines, and other growth factors as well as changes in the mechanical properties of the ECM[64,68,80]. This activated fibroblast, now called a myofibroblast, will have altered expression of a number of proteins not normally expressed in fibroblasts, such as α-smooth muscle actin. Expression of this protein will result in a smooth muscle-like contractile cell[64,68,80]. Myofibroblasts, also, begin to synthesize and secrete increased levels of collagen and chemical factors that will further promote tissue fibrosis[11,35,36,50,64,68,80,82].

Fibroblast to myofibroblast conversion occurs as a result of re-expression of developmental genes to cause an enhanced remodeling of the ECM, particularly in pathologies, such as post myocardial infarction, or MI[11,24,64]. Thus, the phenotype of

myofibroblasts are different than the fibroblasts in that myofibroblasts are thicker cells with ruffled membranes along with highly active endoplasmic reticulum[6,24,64]. Myofibroblasts are distinguishable from fibroblasts due to their high level of exocytotic vesicles and stress fibers[6,24,64]. These changes in morphological characteristics lend myofibroblasts to have different functional characteristics than that of fibroblasts[6,24,64]. Functions and characteristics include the ability to contract collagen gels, are more mobile than "normal" fibroblasts and will express contractile proteins, such as α-smooth muscle actin[6,24,64]. All of which are considered to be important for wound closure and structural integrity of healing scars[6,24,64]. Myofibroblasts have demonstrated to play a significant role in reparative fibrosis of an infarcted heart[6,24,64].

Myofibroblasts, while initially beneficial in pathologies requiring enhanced scar formation to maintain organ integrity (e.g., myocardial infarction), become detrimental to organ function if an increased population of myofibroblasts persists[6,24,64]. Unchecked increases in myofibroblasts are capable of producing collagenous barriers between myocytes and inhibit the conduction of excitable signals responsible for keeping the heart beating properly[6,24,64]. Studies have demonstrated an increased deposition of the ECM or fibrosis due to the high glucose levels seen in diabetic patients, which is thought to deleteriously impact myocardial function[6,11,24,64,82]. Myofibroblasts have specialized adhesion complexes called fibronexus or mature local adhesion[6,11,24,64,82]. These are microfilament bundles that terminate at the cell surface allowing for the formation of a bridge between the internal microfilaments of a myofibroblast and ECM component domains[6,11,24,64,82]. This functions as a contractile mechanism enabling these cells to generate force on the surrounding ECM[6,11,24,64,82]. Chronic exposure to increased

mechanical and chemical stimulation results in elevated levels of collagen[6,11,24,64,82]. This process may occur as a result of an increase in collagen gene transcriptional activity through elevated cascade activity[27], changes in transcriptional levels of MMPs to decrease degradation[67], as well as changes in post-transcriptional regulation of ECM proteins[21].

In normal, healthy cardiac tissue, myofibroblasts are usually not present; however, myofibroblasts appear in the myocardium, arising from interstitial and adventitial fibroblasts, because of injury[6,11,24,64,82]. At the site of injury, chemokines are released and myofibroblasts migrate towards and become highly responsive to such local components[6,11,24,64,82]. Myofibroblasts will then begin to secrete high levels of ECM proteins, such as collagen, to aid in wound healing[75]. During normal wound healing, myofibroblasts undergo apoptosis after stabilizing the wound[75]. Deviations in the wound healing process can prevent apoptosis from occurring resulting in a sustained myofibroblast population secreting collagens to produce a fibrotic state[75]. Ultimately, high populations of myofibroblasts persisting in the myocardium will be more detrimental due to playing a critical role in cardiac pathology and remodeling [6,11,24,64,82]. In certain pathologies, such as diabetes mellitus, fibroblast activation to myofibroblasts and myofibroblast apoptosis are not properly regulated due to increased mechanical and chemical signals resulting in a maladaptive tissue remodeling[6,11,24,64,75,82].

Advanced glycation end-products (AGEs)

AGEs are the products of non-enzymatic glycation and oxidation of proteins, lipids, and nucleic acids in the presence of sugars, which accumulate in differing pathological situations, such as diabetes, inflammation, renal failure, and aging[31,52].

AGEs crosslink with long-lived protein, such as collagen, providing structural rigidity to the ECM[83]. However, too much of an increase in AGEs, such as in a diabetic environment, can lead to an alteration in tissue function[31,52,83]. AGEs are also capable of modulating multiple cellular processes via binding to their cell surface receptor, known as the receptor for AGEs or RAGE[31,52,83].

AGEs are a variety of heterogeneous compounds that are formed through a process called the Maillard reaction[31,61,80]. The starting compounds that undergo the Maillard reaction consist of proteins, lipids, and nucleic acids, which are subsequently glycated or oxidized non-enzymatically[31,61]. Due to high concentrations in human plasma, especially in a diabetic environment, glucose plays a primary role in the glycation process[31,61]. The beginning of the Maillard reaction consists of an interaction between the carbonyl groups of a reducing sugar, such as glucose and amino acid[31,61,80]. Cysteine, lysine, and histidine are the preferred amino acid substrates; however, arginine and tryptophan can also be sites of production of a Schiff base[46]. Creation of the Schiff base usually takes only a few hours to occur and is reversible[31], however, since Schiff bases are rather unstable, they convert into more stable compounds known as Amadori products. Production of Amadori products through molecular rearrangements occurs over a much longer time period, usually weeks to months[31,61]. The Amadori products then undergo a series of reactions, which occurs over months and years, to produce permanent structural changes via oxidation, dehydration, and degradation to yield the highly stable AGE compounds[31,61]. The process of AGE formation is depicted in Figure 1.1. AGE formation and accumulation will occur in the presence of a hyperglycemic environment.

Therefore, in diseases in which hyperglycemia is prevalent, such as in diabetes mellitus, there is an increase in AGE cross-linked products[31,52,61,83].

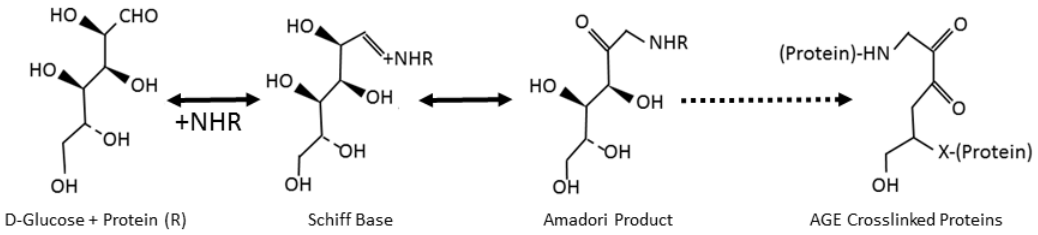

Figure 1.1 Formation of advanced glycation end-products (AGEs).

AGEs undergo a non-enzymatic process called a Maillard reaction involving glucose and proteins leading to the formation of a Schiff base; this process occurs over a few hours and is reversible. Schiff bases are highly unstable and convert to a more stable compound, an Amadori product. Amadori products undergo several reactions, over a timespan of months to years, to produce permanent structural changes via oxidation, dehydration, and degradation to produce the final, highly stable AGE compound.

Receptor for AGEs (RAGE)

After an AGE is formed, it binds to its receptor, which is called receptor for advanced glycation end-products or RAGE[42,63], activating the AGE-RAGE signaling pathway. RAGE is a member of the cell surface receptor immunoglobulin superfamily and is a key element of the innate immune system[23,42,63]. More specifically, RAGE is involved in the onset and sustainment of the inflammatory response[23,42]. RAGE is a pattern recognition receptor which recognizes common features of molecules rather than a specific ligand[23,42]. Thus, RAGEs have been demonstrated to bind to multiple AGE isoforms including carboxymethyl lysine (CML) and carboxyethyl lysine (CEL) as well as additional ligands aside from AGEs, such as the S100 calgranulins, which is a family of calcium binding proteins, amyloid-beta peptides, and extracellular high mobility group

box-1 (HMGB1)[42,63]. Pattern recognition receptors identify pathogen-associated molecular patterns, or PAMPs, which are associated with microbial pathogens, damage-associated molecular patterns (or DAMPs), or cellular stress[23,42,60].

RAGE is composed of three domains: extracellular, transmembrane, and short cytoplasmic[23,42,63]. The extracellular region of RAGE consists of two subdomains, which includes one variable (V), critical for ligand binding, and two constant (C1 and C2)[23,42,63]. The V subdomain of RAGE is the N-terminal immunoglobulin domain located farthest from the plasma membrane whereas the C2 subdomain is closest to the membrane[23,42,63]. A slightly bent elongated structure is formed where the V and C1 subdomains are joined[23,42]. The V and C1 subdomains are fixed as a whole structural unit, called VC1, whereas the VC1 and C2 subdomains are attached together forming a flexible linker between the two subdomains[23,42]. AGE-modified BSA and S100B have been shown to bind to VC1[23,42].

AGE-RAGE Signaling Cascade

AGE-RAGE activity has been demonstrated to be increased in a hyperglycemic environment such as in diabetes mellitus, promotes the synthesis of AGEs and increased RAGE expression[31,35,52,61,83]. The overall pathological effects associated with the AGE-RAGE cascade in diabetes mellitus include increased RAGE expression as well as increased fibroblast differentiation and increased collagen production[31,35,36,52,61,83]. Elevated AGE-RAGE cascade activation creates a forward cycle that leads to an increased collagen production and a loss of collagen degradation by matrix metalloproteinases (MMPs) resulting in fibrosis[31,35,36,52,61,83]. Cardiac fibrosis also leads to an alteration of tissue in regards to mechanical and functional properties[31,35,36,52,61,83].

For example, in the heart, fibrosis led alterations of mechanical properties result in diastolic dysfunction and a decreased cardiac output, which accompanied advanced AGE accumulation[31,35,36,52,61,83] as well as increased myofibroblast populations[35,61,77,83].

The AGE-RAGE signaling cascade has been found in numerous tissues of the body including kidney, heart, lung, brain, and skeletal muscle[31,35,52,61,63,77,83]. Soman et al. (2013) demonstrated that RAGE has been involved in diverse diseases including arthritis, cancers, neurological disorders, cardiovascular disorders, and diabetes. This pathway disrupts normal function of the tissue or cell, such as in the heart, by the interaction of AGE with its receptor, RAGE, leading to an accumulation of free radicals[63,77]. Further evidence demonstrates that the AGE-RAGE cascade found in a diabetic environment increases reactions of oxidative stress and inflammation leading to vascular damage and related complications[52,63,77]. Reactive oxidative stress (ROS) is increased by AGEs through multiple mechanisms including decreased glutathione stores, diminished activities of catalase and superoxide dismutase (SOD), and through activation of protein kinase C (PKC)[52,63,77]. Also, according to Ramasamy, R., et al. 2011, ligand-RAGE binding alters cellular function and leads to increasing AGE synthesis and accumulation, which are characteristics of multiple diabetic problems, as well as increased inflammation and tissue stress.

Inflammatory responses due to the AGE-RAGE interaction can be explained by an increase of production of proinflammatory cytokines such as interleukins, TNF-α, and monocyte chemotactic protein (MCP-1) to amplify the inflammatory response [11,35,45,65,82]. Studies have shown that increased synthesis of AGEs results in an increase in RAGE expression due to an autocrine response[42,45]. It is the increase of ligand-induced RAGEs

in pathological conditions, such as diabetes mellitus, inflammation, oxidative stress, renal failure, and Alzheimer's disease that leads to the increased severity of these diseases[45,52,77]. In diabetes mellitus, the AGE-RAGE signaling pathway downstream mechanisms contribute to cell stress, cellular dysfunction, and damage of target organs, all of which leads to diabetic complications[42,45,52,53,77,83]. In pathologies such as diabetes mellitus, we know that AGE accumulation is a result of a hyperglycemic environment, and when AGEs are bound to their receptor, RAGE, AGE-RAGE cascade activation can elicit multiple downstream signaling events coupling extracellular signals into activation of intracellular pathways[42,45,52,53,83]. Activation of intracellular pathways includes PKC-ζ signaling.

PKC-ζ signaling

The multiple outcomes of AGE-RAGE signaling have been proposed to operate indirectly through protein kinase C (PKC)[79,83]. PKC activity and subsequent activation of prostaglandins, cytokines, and ECM protein expression was increased in cell culture experiments to model type I and type II diabetes mellitus hyperglycemic growth conditions, *in vitro*[72,83]. PKC kinase family members are grouped based on their second messenger requirements. There are three groups of PKC isoforms: conventional, novel, and atypical[2,72,83]. The conventional PKC family is activated by calcium, phosphatidylserine, diacylglycerol, or phorbol-12-myristate-13-acetate and includes PKC-α, -β I, -β II, and -γ[2,72,83]. The novel PKC family is activated by phosphatidylserine, diacylglycerol, or phorbol-12-myristate-13-acetate and includes PKC-ε, -δ, -η, and -θ[2,72,83]. The atypical PKC family cannot be activated by any of the previously mentioned

second messengers[83] however, phosphatidylserine has been shown to activate atypical PKC isoforms in some cases[2,72]. The isoforms in the atypical PKC family include -ζ and -ι/λ[2,72,83].

To date, deviations of vascular cell homeostasis have been shown to be mediated through different PKC isoforms[83]. More specifically, the activation of PKC isoforms have been associated with alterations of the vascular such as increased permeability, contractility, ECM synthesis, cell growth, and apoptosis[83]. The demonstrated PKC isoforms were PKC-β and PKC-ζ in aortic and cardiac tissue of diabetic mice. However, PKC-ζ has been identified as the most plausible target for RAGE phosphorylation through additional examination of multiple PKC isoforms. PKC-ζ is involved with activating downstream cascade pathways leading to activation of mitogen-activated protein kinase (MAPK)[83].

Numerous cell processes including development, phenotype differentiation, and ECM protein synthesis are areas where the MAPK family plays an important role[44,62,83]. Members of the MAPK family are extracellular-signal-regulated kinases (ERKs), ERK5, c-JunNH2-terminal kinases (JNKs) and the p38 MAP kinases[54,62]. In a study by Koya et al. (2000), ERK, a subfamily of MAPKs, can be activated through a PKC-dependent pathway. ERKs are involved in cell signaling cascades responsible for cell differentiation and proliferation[62,83]. ERK1 and ERK2, are 84% identical and share many functions [44,54,62] and are commonly referred to as ERK1/2 due to being so similar[54,62]. Roles of ERK1/2 consist of a very broad range with a few being, at the cellular level, a modulator in cell cycle proliferation, cytokinesis, transcription, and differentiation[44,54,62]. In addition, ERK1/2 also modulates cell death, GAP junction formation, actin and microtubule

networks, and cell adhesion[54,62]. At the physiological level, ERK1/2 is required for development of the heart and immune system, antigen activation, and memory formation as well as responses to various growth factors, hormones, and insulin; however, ERK1 knockout mice have a generally normal phenotype, but ERK2 knockout mice are embryonic lethal[44,54,62]. When there is abnormal signaling of ERK1/2, it can cause many pathologies including accelerating viral infection, many cancers, diabetes, and cardiovascular disease[54].

Growth factor receptors, integrins, tyrosine kinases Src and Fyn as well as others, and G-protein coupled receptors can all activate MAPK[54,62]. Phosphorylation of ERK occurs at the plasma membrane but can also be on endomembranes[54]. ERK1/2 activation requires Raf, a molecular switch, to create a stepwise serine kinase cascade. This begins with activation of Raf leading into activation of MAPK kinase kinase, MAPK kinase, MAPK, and ERK[62,81,83]. Once ERK is activated, it is able to translocate into the nucleus leading to the activation of transcription factors initiating cellular proliferation, differentiation, and matrix accumulation[54,62,81,83].

Both independently as well as synergistically, AGE-RAGE and PKC-ζ signaling cascades have been shown to increase ERK activation[79,83]. Thus, PKC-ζ serves as a common mediator of these two different cascades[79,83]. A requirement to generate AGE-RAGE signaling, RAGE must be phosphorylated at Ser391 and PKC-ζ has been known to phosphorylate Ser391 of the intracellular RAGE domain[58,83]. In order for this to occur, however, PKC-ζ must be activated by Ras, a small GTPase[58,83]. In that case, the conversion of extracellular signals into intracellular signaling pathways of the AGE-RAGE cascade may be made possible via a small GTPase protein, like Rap1a[37,58,81,83].

Rap1a-A Small GTPase

Rap1a is a member of the small GTPase superfamily, of which there are more than a hundred proteins classified based on their structure, sequence, and function. This superfamily can be further subdivided into six groups or families, which include Ras, Rho, Rab, Arf, Ran, and Kir/Rem/Rad[20]. Rap1a is a member of the Ras GTPase family. There are multiple isoforms, encoded by various independent genes, of the Rap protein existing in higher and more complex organisms[9,37]. These isoforms of Rap are known as Rap1a, Rap1b, Rap2a, Rap2b, and Rap2c[9,37]. Rap1a and Rap1b, referred to as Rap1 and share a >90% sequence homology[37]. Rap2a, Rap2b, Rap2c, referred to as Rap2, are 65-70% homologous to Rap1[37]. Rap1 was hypothesized in previous studies as a direct inhibitor of Ras by competing for the same effector proteins[37]. However, further studies discovered that both Rap1a and Rap1b are functionally different from Ras and are thought to be involved in vastly different signaling pathways, particularly in the cardiovasculature[37]. Extracellular-intracellular signaling to integrins, formation of focal adhesion, and cell adhesion increases have all been established with the activation of Rap1[37]. Rap1a or Rap1b knockdown in cultured human microvascular endothelial cells appears to decrease extracellular matrix adhesion as well as impair cell migration and increases permeability[37].

Multiple pathways that regulate cell adhesion, proliferation, and cell migration are regulated by Rap effector proteins in the cardiovasculature[37]. More specifically, when the AGE-RAGE signaling pathway is activated there are three significant outcomes, which include fibroblast differentiation, RAGE expression, and collagen production. This pathway, in reference to fibroblasts, allow for the increased production of collagen or

fibrosis[82]. Also, elevated glucose levels, which result in increased cAMP-PKA-Rap1a signaling, can also impact the fibroblast-ECM interactions thus the migration and contractility due to the alteration of the expression of specific integrin proteins[82].

Rap1a Signaling Cascade

G-protein coupled receptors (GPCRs), or 7-transmembrane receptors, are a large group of receptors that use G-proteins as necessary components of signal transduction. GPCRs are made up of three different components: the ligand-binding subunit (receptor), the G-protein (guanine nucleotide-binding proteins), and the effector (enzyme or second messenger)[55]. The ligand-binding subunit (receptor) consists of three domains including extracellular, transmembrane, and intracellular. The intracellular domain, generally an intracellular loop between the fifth and sixth transmembrane domain of a seven transmembrane receptor, as well as the carboxyl terminus contains phosphorylation sites for G-proteins[55]. Binding of an agonist to the GPCR results in a conformation change in the receptor that is transmitted to the bound G-protein[18]. G-proteins, or guanine nucleotide-binding proteins, are a family of proteins that act as molecular switches within the cells, transducing signals from the exterior of the cell to its interior[5,37,66]. Activity of G-proteins is controlled by factors that regulate their ability to bind to and hydrolyze guanosine triphosphate (GTP) to guanosine diphosphate (GDP)[5,37,66]. When bound to GTP, G-proteins are 'on', and, when bound to GDP, they are 'off'[6,37,66]. There are two different families of G-proteins: 1) heterotrimeric or large G-protein and 2) monomeric or small G-proteins.

Heterotrimeric G-proteins, or large G-proteins, are activated by GPCRs and composed of an α, β, and γ subunits[34,55]. When the GPCR conformation occurs as a result

of ligand binding, adenylyl cyclase, a G-protein coupled receptor (GPCR) effector enzyme, synthesizes cAMP from adenosine triphosphate (ATP) as a response to first messengers such as hormones, neurotransmitters, and various environmental stimuli[22,55]. The activated G_α subunit exchanges GTP in place of GDP which causes the dissociation of G_α subunit from the $G_{\beta\gamma}$ dimer as well as from the receptor. The dissociated G_α and $G_{\beta\gamma}$ subunits interacts with other intracellular targets to propagate the signal transduction cascade while the freed GPCR is able to rebind to another G-protein[16]. The intracellular second messenger cAMP is coupled to PKA activation as well as other downstream signaling events[37]. cAMP-dependent protein kinase (PKA) is a homologous ligand-activated kinase and the main intracellular receptor for cAMP[22]. Once PKA is activated by bound cAMP, PKA catalyzes the transfer of the γ–phosphate of ATP to select serine or threonine residues in many cellular proteins[22]. In addition to PKA signaling, cAMP has the ability to activate other cell signaling pathways. A second pathway activated by cAMP is the Ras GTP superfamily binding proteins Rap1 and Rap2 via the Exchange Protein Activated by cAMP or EPAC[36,37].

Monomeric G-proteins, or small G-proteins (20-25 kDa), belong to the Ras superfamily of small GTPases. These proteins are structurally and functionally homologous to the G_α subunit found in heterotrimers in that they also bind GTP and GDP and are involved in signal transduction[34]. Rap1a, a small monomeric G-protein, acts as a molecular switch coupling extracellular events to intracellular signaling[37,66]. Cycling of inactive to active Rap1a is facilitated by the releasing of the GDP molecule and binding of the GTP molecule via a guanine-nucleotide-exchange factor (GEF)[5,37,66]. Active Rap1a cycles off via the GTPase-activating-protein (GAP) which hydrolyzes the GTP molecule

into GDP[5,17,37,66]. Examples of GEFs include C3G, CalDAG-GEF, RasGRP2, PDZ-GEF1, PDZ-GEF2, and PLCε[17,37]. In the cardiovasculature, however, the most well described GEFs that activate Rap1a are known as exchange proteins directly activated by cyclic AMP1 and 2 (EPAC1 and 2)[17,37]. Binding of cAMP to EPAC creates a conformation change allowing it to catalyze nucleotide exchange of Rap1[17,37]. The cycling process of Rap1a is not only triggered by EPAC, but can also occur indirectly by other second messenger molecules such as calcium or diacylglycerol[17,37]. All three of these second messenger molecules are components of the protein kinase A (PKA) signaling cascade[17,37]. The cycling of Rap1a is illustrated in Figure 1.2 below.

As an overview, after initial activation of the AGE-RAGE signaling cascade, Rap1a activation and signaling starts with a first messenger ligand activating its receptor leading to activation of adenylyl cyclase which synthesizes cAMP. cAMP binds to PKA, activating PKA, leading to downstream activation of EPAC and Rap1a[17,22,37,55,66]. Next, Rap1a is proposed to operate through PKC-ζ leading to activation of downstream players of AGE-RAGE signaling cascade, as illustrated in Figure 1.2 below. Activation of cAMP/PKA-Rap1a leads to three known outcomes of the AGE-RAGE cascade including fibroblast differentiation, increased RAGE expression, and collagen production[83].

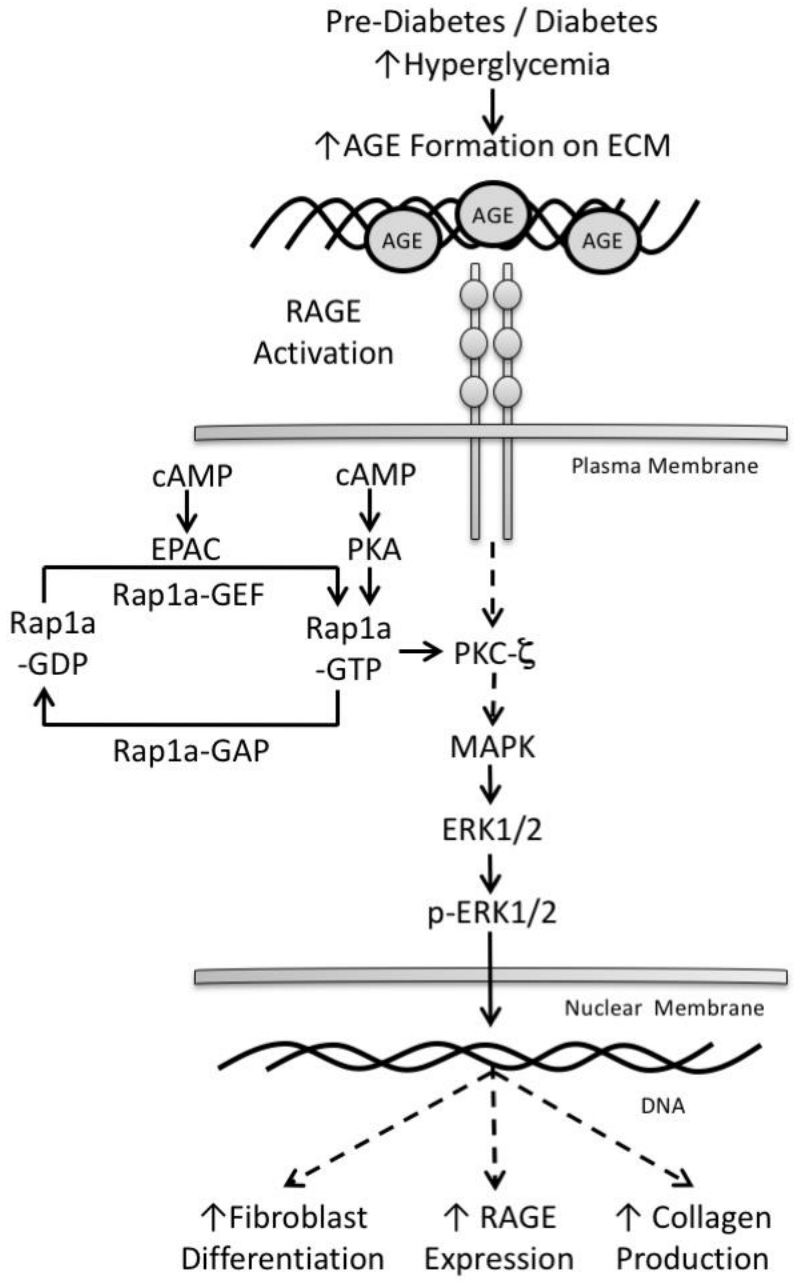

Figure 1.2 Representative of AGE-RAGE and cAMP/PKA-Rap1a signaling cascades.

Hyperglycemia, with pre-diabetes or diabetes, increases the crosslinking of structural protein collagen with the excessive glucose increasing the rate of advanced glycation end-product (AGE) formation on extracellular matrix. AGEs bind to their receptor, receptor for advanced glycation end-products (RAGE), creating the initial activation of AGE-RAGE signaling cascade. Rap1a signaling begins with a first messenger ligand activating its receptor which will stimulate synthesis of cAMP by adenylyl cyclase. cAMP activates protein kinase A (PKA) and the exchange protein directly activated by cAMP (EPAC) activating Rap1a. Rap1a is proposed to operate through protein kinase C-ζ (PKC-ζ) in the AGE-RAGE signaling cascade leading to activation of mitogen-activated protein kinase (MAPK) and transcription factor extracellular signal-regulated kinase 1/2 (ERK1/2) to create three known outcomes: increase in fibroblasts differentiation into myofibroblasts, increase in RAGE expression, and increase in collagen production.

Diabetic Animal Model

Adipocytes primarily secrete leptin; leptin signaling promotes communication to the central nervous system (CNS) when there is an abundance of available energy stores to decrease food intake and induce energy expenditure[78]. The diabetic animal model used in these studies was the *Lepr^{db}* (db-/- or commonly called db/db) type II diabetes mellitus mice (BKS.Cg-*Dock7^{m}* +/+ *Lepr^{db}*/J, Jackson Labs). The *Lepr^{db}* leptin receptor mutation is a G→T point mutation that results in nonfunctional leptin receptors[76,85]. This point mutation creates a donor splice site leading to abnormal splicing and the insertion of 106 nucleotides leading to expression of a premature stop codon[76,85]. This mutation occurs at the longest and most important of five leptin receptor isoforms, the Ob-Rb isoform[76,85]. With the leptin receptor mutation, the leptin receptor is insensitive to leptin signaling meaning no communication is provided to the CNS that there are abundant energy stores and to decrease food intake; eventually leading into obesity and insulin resistance[78]. These mice develop hyperglycemia by 8-weeks of age, overt diabetes by 12-weeks of age, and exhibit many common features of type II diabetes mellitus including hyperlipidemia, obesity, and insulin resistance. At 16-weeks of age, the animals were sacrificed for cell culture and biochemical assays.

Background of Pharmacological Cell Treatments

Isoproterenol

Isoproterenol (ISO), also known as isoprenaline, is a catecholamine compound and non-selective β-adrenergic receptor agonist used in cardiovascular research[84]. ISO increases the amount of cytosolic cAMP, activating PKA in turn, and eventually increasing Rap1a activation[84]. ISO increases Rap1a activation by first activating the β-

adrenergic receptor, which is a G-protein-coupled receptor, which activates the G-protein, G_s, by disassociating the bound ADP and binding of ATP[84]. This activation of G_s leads to activation of adenylyl cyclase[84]. Adenylyl cylcase synthesizes cAMP which activates PKA and EPAC pathways leading to the downstream activation of Rap1a[84].

8-CPT-2Me-cAMP

8-CPT-2Me-cAMP or also known as an EPAC Agonist (EPAC Ag) directly and specifically activates Rap1a for gain-of-function studies[39]. EPAC Ag is a selective activator of EPAC1 which is the cAMP-sensitive guanine nucleotide-exchange factor necessary for Rap1a activation both *in vitro* and *in vivo*[39].

Rap1a siRNA

Small interfering RNAs (siRNAs), also referred to as silencing RNAs, are double-stranded RNA molecules approximately 20-25 base pairs in length. siRNA will bind to the complementary mRNA sequences of specific genes and restrict the post-transcriptional translation and expression of the RNA[1,19,28]. Introduction of double-stranded RNA will result in the degradation of targeted mRNAs in the cytoplasm to effectively silence gene activity by reduction mRNA transcript necessary for production of target proteins[1,19,28]. To diminish effectively transcription and translation of a target gene, siRNA must first enter into the cell. Prior to incubating the siRNA with the cells, the siRNA will be enclosed within a lipid vesicle (lipofectamine) to allow passage into the cells. Once inside the cells, the siRNA will bind to the complementary mRNA nucleotide sequences of specific genes targeting them for degradation by ribonuclease III (RNase III)[1,70]. The degraded double stranded RNA will then associate with the RNA-

Induced Silencing Complex (RISC). Once bound Argonaute, a RISC protein, will be activated and cleave the mRNA to interfere with the transcriptional and translational process of a specific gene[1,29,70].

PKC-ζ Pseudo-substrate

PKC-ζ Pseudo-substrate (PS) is a selective, reversible inhibitor of PKC-ζ in the group Ser/Thr protein kinase inhibitors[59]. PKC-ζ PS is a substrate-competitive inhibitor meaning that it competes with the usual substrate to bind to PKC-ζ[59]. PS is able to bind to PKC-ζ but does not activate it by creating conformational change. Therefore, signaling through PKC-ζ is not activated.

AGE-BSA

Advanced glycated end-products-bovine serum albumin (AGE-BSA) is a RAGE agonist activating RAGE receptor by increasing the amount of AGEs present. AGE-BSA is produced by reacting BSA with glycolaldehyde leading into formation of AGEs via the Maillard reaction leading into formation of Amadori product and the final, stable compound AGE as previously discussed[4]. In the following sections, AGE-BSA will be referred to as AGE.

Specific Aims

The molecular mechanisms regarding changes in fibroblasts during type II diabetes mellitus are not well understood. The purpose of this study was to identify and confirm components of the PKA-dependent Rap1a signaling participate in the AGE-RAGE cascade. Therefore, we hypothesized that the downstream effects of AGE-RAGE signaling in diabetes mellitus were increased by Rap1a GTPase via a PKA-dependent pathway resulting in elevated ECM accumulation and remodeling in the heart. The following specific aims were used to test the hypothesis and are shown in Figure 1.3.

Specific Aim 1

Define a link between PKA and AGE-RAGE signaling cascades, *in vitro*. We hypothesize that the AGE-RAGE signaling cascade can operate in a PKA-dependent manner to activate Rap1a to stimulate downstream mediators, such as ERK1/2. Gain-of-function and loss-of-function experimental designs were used, *in vitro*, to evaluate the changes in fibroblast phenotype and RAGE activation. Lean, non-diabetic control (Het) and genetically diabetic (db/db) mice were used to determine the mechanistic relationship between Rap1a and the AGE-RAGE signaling cascade.

Specific Aim 2

We will determine if changes in Rap1a GTPase expression affect PKA dependent diabetes-mediated AGE-RAGE signaling *in vitro*. We hypothosize that Rap1a is a key mediator in PKA-dependent AGE-RAGE signaling. By using gain-of-function experiments to stimulate Rap1a activity via EPAC activator and loss-of-function approaches using Rap1a siRNA in cultured cardiac fibroblast cells from lean, non-

diabetic (Het) and diabetic (db/db) mice, we can better define a mechanistic role for Rap1a in PKA-dependent AGE-RAGE signaling. Rap1a hyperactivation was expected to stimulate increases in AGE-RAGE signaling cascade independent of PKA, leading to subsequent fibroblast phenotype changes and RAGE up-regulation. Loss-of-function studies were expected to decrease AGE-RAGE signaling cascade outcomes limiting fibroblast phenotype changes and RAGE expression.

Significance

The successful completion of this project will define a cellular and molecular mechanism for PKA mediated Rap1a activation in AGE-RAGE-dependent myocardial remodeling. These studies are the first of its kind to provide Rap1a as a unique target for therapeutic strategies aimed at reducing chronic hyperglycemia-mediated ECM production and accumulation in diabetic patients.

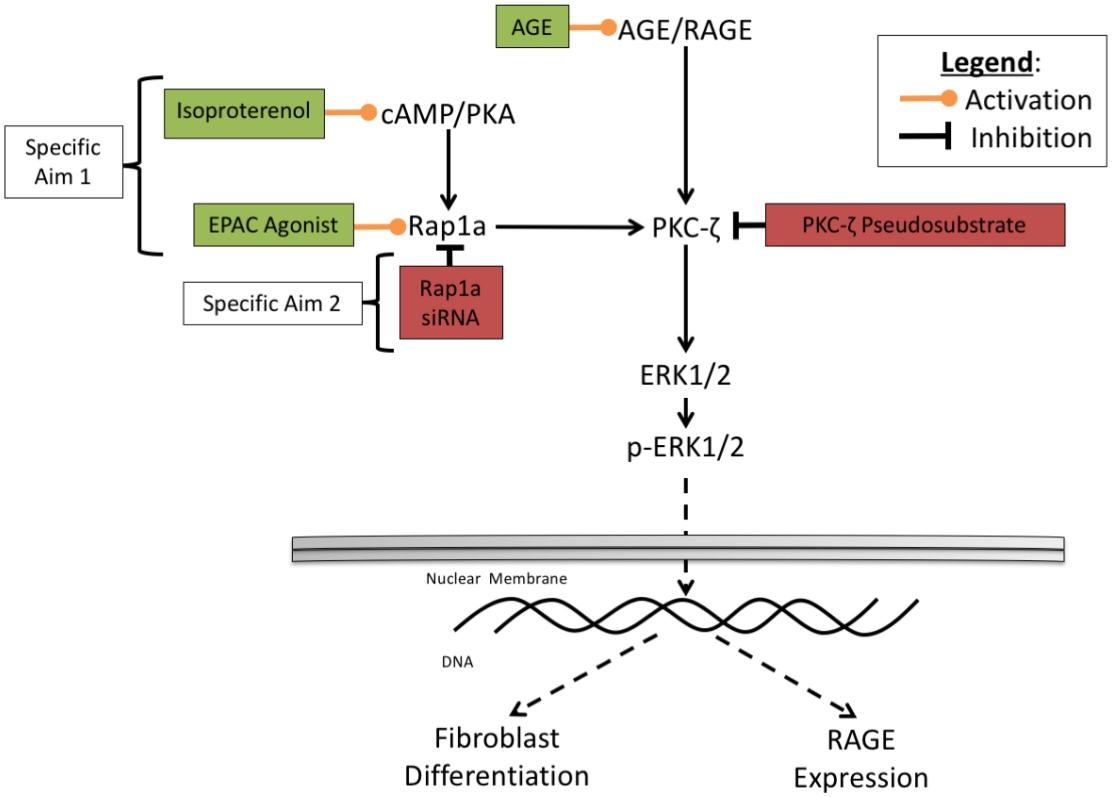

Figure 1.3 Schematic representation of specific aims

In Specific Aim 1, Rap1a was indirectly activated through activation of cAMP/PKA via Isoproterenol (ISO) treatment as well as directly activated Rap1a through 8-CPT-2Me-cAMP (EPAC Ag) treatment. In Specific Aim 2, Rap1a expression was reduced with Rap1a siRNA treatment. For both aims, glycated albumin (AGE) and PKC-ζ Pseudo-substrate (PS) were used to robustly activate the AGE-RAGE signaling axis and block PKC-ζ signaling, respectively. The green boxes (ISO and EPAC Ag) with an orange line mean activation and red boxes with a black line (Rap1a siRNA and PS) mean inhibition.

CHAPTER II

MATERIAL AND METHODS

Animal Model

The animal model for all experiments was 15-16 week old male genetically induced diabetic mice (C57BL/KsJ-db/db) and heterozygous (Het) lean littermates were used as controls. The genetically diabetic mice have a leptin receptor mutation and are known as *Lepr^{db}* (db/db) type II diabetes mellitus mice (BKS.Cg-*Dock7^{m}* +/+ *Lepr^{db}*/J, Jackson Labs). The mice were housed under standard environmental conditions and maintained on commercial mouse chow as well as tap water ad libitum. All studies followed the principles of the National Institutes of Health "Guide for the Care and Use of Laboratory Animals," (NIH publication No. 85-12, revised 1996) and the protocol was approved by the Mississippi State University Animal Care and Use Committees (IACUC protocol number 14-046). At 15-16 weeks of age, mice were euthanized using carbon dioxide inhalation. The chest was opened and the heart quickly excised for further cellular and biochemical experiments.

Cell Isolation

Cardiac fibroblasts were isolated using a modified protocol by Burgess et al.[10,13]. The mice were sacrificed and ventricles of heart were dissected from extra-cardiac tissue and atria. Ventricles were minced into 2 mm pieces and rinsed with ice cold sterile phosphate buffered saline. Ventricles were digested for 10 minute intervals with type II

collagenase (240 U/mg; Worthington Biochemical) supplemented with 0.25% Trypsin (Life Technologies) in a water-jacketed spinner flask. After 10 minutes, the supernatant was collected in a sterile 50 mL tube and a stop buffer of Dulbecco Modified Eagles Medium (DMEM) containing 20% Fetal Bovine Serum (FBS) was added to quench the collagenase. A 10-minute 200 xg centrifugation step was performed to pellet isolated cells. Cells were resuspended and maintained in DMEM (CellGro) containing 15% FBS, 1X L-glutamine (Fisher Science), and 2X Primocin® antibiotic and antimycotic (Fisher Science). Starting again with the 10-minute enzyme incubation, the isolation process was repeated until all myocardial tissue was digested. Cells were plated on 60 mm dishes and isolated fibroblasts were purified by selective attachment to tissue culture plastic. Fibroblasts from diabetic animals were maintained in a high glucose DMEM (4.5 g glucose/L) and non-diabetic fibroblasts were grown in a normoglucose DMEM (1 g glucose/L). All studies used fibroblasts at P0-1 for signaling experiments. Fibroblasts were passaged prior to 95% confluency, following detachment with a 0.25% trypsin/0.1% ethylenediaminetetraacetic acid (trypsin/EDTA) solution (Life Technology). Hearts from 2-3 mice were used per isolation. Data from 4-5 independent isolations were collected per group.

Pharmacological Cell Treatments

Once fibroblasts reached 90-95% confluency, the fibroblasts were serum starved for 24 hours in 0.01% FBS DMEM media to yield quiescent fibroblasts. Following serum starvation, the media was changed and the fibroblasts were allowed to rest for 1 hour. The fibroblasts were then treated with Isoproterenol (ISO) (Sigma Aldrich; 10 μM in PBS), 8-CPT-2Me-cAMP (EPAC Ag) (Sigma Aldrich; 100μM in PBS), Rap1a siRNA

(sc-41853) or scramble siRNA control (sc-37007) (Santa Cruz Biotechnology; 10 µM siRNA in Transfection Reagent [sc-29528]) as well as with (+) or without (-) PKC-ζ pseudo-substrate (PS) (Sigma Aldrich; 1 µg/mL in PBS) for 24 hours. These groups of fibroblasts were then treated with glycated albumin (AGE) (Sigma Aldrich; 0.5 mg/mL in PBS) for an additional 24 hours prior to harvesting. A timeline of the fibroblast pharmacological cell treatments, which has been described above, is shown in Figure 2.1.

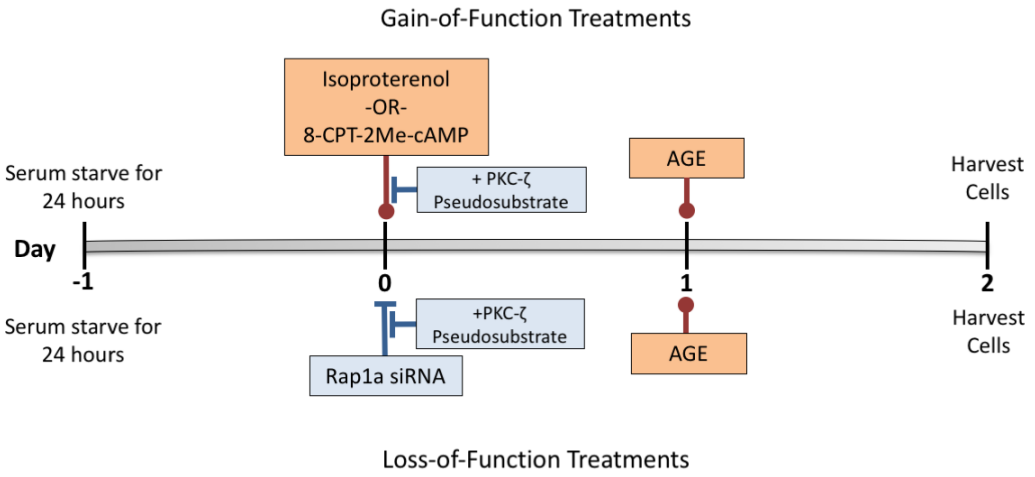

Figure 2.1 Timeline of fibroblast cell treatments

Fibroblasts at 95% confluency were serum starved for 24 hours with 0.01% Fetal Bovine Serum (FBS) Dulbecco Modified Eagles Medium (DMEM) on day -1. On Day 0, fibroblasts were treated with Isoproterenol (ISO), 8-CPT-2Me-cAMP (EPAC Ag), Rap1a siRNA or scramble siRNA control as well as with (+) or without (-) PKC-ζ Pseudo-substrate (PS). Following 24 hours, Day 1, fibroblasts were treated with AGE. After another 24 hours, Day 2, fibroblasts were harvested.

Protein Isolation

Fibroblasts were harvested and proteins isolated as follows: Conditioned media was removed, frozen, and stored at -80°C until biochemical assays could be performed. The culture dishes with adherent fibroblasts were washed 1X with ice cold PBS and the PBS was vacuum aspirated off the plates. 200 µL of modified Hunter's Buffer, containing 1% Triton X-100, 75 mM NaCl, 5 mM Tris pH 7.4, 0.5 mM orthovanadate, 0.5 mM EDTA, 0.5 mM EGTA, 0.25% NP-40 and protease inhibitors, was added to the plates on ice. After 10 minutes, the fibroblasts were scraped off and transferred to 1.5 mL centrifuge tube. The fibroblasts were probe-sonicated for 5 seconds while on ice and centrifuged for 15 minutes at 20,000 xg at 4°C. After the samples were centrifuged, the supernatant was transferred to new 1.5 mL centrifuge tubes and stored at -80°C**.**

The concentration of proteins in each sample was determined using the bicinchoninic acid (BCA) assay (Pierce Biotechnology) according to manufacturer's instructions. A standard curve was generated using serial dilutions of bovine serum albumin (BSA) from 2.0 mg/mL to 0.0 mg/mL to interpolate the concentration level of sample proteins based on the optical density (OD) of the spectrophotometer reading (λ=462 nm) using GraphPad (Prism 5 Software).

Western Blot Analysis

Equal amounts of protein lysate (25-50 µg) were separated on a 10% sodium dodecyl sulfate (SDS)-polyacrylamide gel (BioRad Laboratories) for approximately 2-3 hours at 100 V at 4°C. Proteins were electrophoretically transferred to nitrocellulose membranes for approximately 18 hours at 100 mA at 4°C. Blots were stained with Coomassie Brilliant Blue Stain (Fisher Scientific) to verify even transfer. Membranes

were blocked in either 5% (1.0 g) powdered milk (for the non-phosphorylated primary antibodies) or 5% (1.0 g) BSA (for the phosphorylated primary antibodies) in 20 mL of TBS-Tween-20 (50 mM Tris, 150 mM NaCl, and 0.1% Tween-20) for an hour and incubated with one of the following primary antibodies overnight at 4°C: cardiac fibroblast phenotype marker α-smooth muscle actin (α-SMA, Sigma-Aldrich), ECM regulators (RAGE, Abcam) and signaling proteins (phospho and total PKC-ζ, Santa Cruz Biotechnologies, phospho and total ERK 1/2, Cell Signaling and Santa Cruz Biotechnologies, respectively; Rap1a, Cell Signaling), while GAPDH (Santa Cruz Biotechnologies) was used to confirm equal loading. A primary antibody (1:1000 ratio [20 µl]) and either 5% (1.0 g) powdered milk (for non-phosphorylated primary antibodies) or 5% (1.0 g) BSA (for phosphorylated primary antibodies) were suspended in 20 mL of TBS-Tween-20 (50 mM Tris, 150 mM NaCl, and 0.1% Tween-20). After the membrane was incubated with a primary antibody overnight at 4°C, membranes were incubated with a secondary antibody for an hour. Secondary antibodies were made using a 1:3000 ratio (0.7 µl) of secondary antibody and either 5% (1.0 g) powdered milk (for non-phosphorylated primary antibodies) or 5% (1.0 g) BSA (for phosphorylated primary antibodies) suspended in 20 mL of TBS-Tween-20 (50 mM Tris, 150 mM NaCl, and 0.1% Tween-20). Depending on which primary antibody used determined which secondary antibody was used: GAPDH (anti-goat), Rap1a (anti-rabbit), phospho-PKC-ζ (anti-rabbit), total-PKC-ζ (anti-rabbit), phospho-ERK1/2 (anti-rabbit), total-ERK1/2 (anti-rabbit), α-SMA (anti-goat), and RAGE (anti-mouse). Blots were developed using Pierce enhanced chemiluminescence (ECL) solution (Pierce Biotechnology), exposed to autoradiography film, and immunoreactive bands were quantified using NIH Image J. To

obtain the graph values in figures, results of Rap1a, α-SMA, and RAGE were normalized to GAPDH, phospho-PKC-ζ was normalized to total-PKC-ζ, and phospho-ERK1/2 was normalized to total-ERK1/2; then those results were normalized to the Universal Control. Normalizing was done, for example, by dividing each signal over the corresponding GAPDH or total (PKC-ζ or ERK1/2) intensity, then dividing that number by the Universal control. GraphPad (Prism 5 Software) was used to provide a graphic representation of results. The nitrocellulose membranes were stripped with stripping buffer (62.5 mM Tris-HCL, 2% SDS, 100 mM 2-mercaptoethanol; pH 6.7) for 10 minutes at 50°C, blocked in either 5% (1.0 g) powdered milk (for non-phosphorylated primary antibodies) or 5% (1.0 g) BSA (for phosphorylated primary antibodies) suspended in 20 mL of in TBS-Tween-20 (50 mM Tris, 150 mM NaCl, and 0.1% Tween-20), reprobed with one of the remaining antibodies, developed, and analyzed as previously mentioned. Immunoreactive bands shown in the results section are from the same series of western blots; meaning that the same membrane was stripped with stripping buffer and reprobed with a different antibody and analyzed as described previously.

Some immunoreactive bands in figures have been re-used in other figures. For example, the immunoreactive band for the Rap1a Control sample shown in Figure 3.1 is also used as the Rap1a Control in Figure 3.2, Figure 3.3, and Figure 3.17. The GAPDH immunoreactive bands shown in Figure 3.1 are the same GAPDH immunoreactive bands as in Figure 3.10 and Figure 3.13. The immunoreactive band for the GAPDH Control sample shown in Figure 3.1 is also used as the GAPDH Control for Figure 3.2, Figure 3.3, Figure 3.10, Figure 3.13, Figure 3.14, Figure 3.15, Figure 3.17, and Figure 3.21. The

GAPDH immunoreactive bands shown in Figure 3.2 are the same GAPDH immunoreactive bands (except for GAPDH Control) as in Figure 3.11 and Figure 3.14. The GAPDH immunoreactive bands shown in Figure 3.3 are the same GAPDH immunoreactive bands (except for GAPDH Control) as in Figure 3.12 and Figure 3.15. The immunoreactive band for the GAPDH Control sample shown in Figure 3.11 is also used as the GAPDH Control for Figure 3.12 and Figure 3.20. The GAPDH immunoreactive bands shown in Figure 3.17 are the same GAPDH immunoreactive bands as in Figure 3.20 and Figure 3.21.

The immunoreactive bands for p-PKC-ζ, t-PKC-ζ, p-ERK1/2, and t-ERK1/2 are used in multiple figures as well; the p-PKC-ζ Control sample shown in Figure 3.4 is also used as the p-PKC-ζ Control for Figure 3.5 and Figure 3.6. The immunoreactive band for the total-PKC-ζ (t-PKC-ζ) Control sample shown in Figure 3.4 is also used as the t-PKC-ζ Control for Figure 3.5, Figure 3.6, and Figure 3.18. The immunoreactive band for the p-ERK1/2 Control sample shown in Figure 3.7 is also used as the p-ERK1/2 Control for Figure 3.8 and Figure 3.19. The immunoreactive band for the total-ERK1/2 (t-ERK1/2) Control sample shown in Figure 3.7 is also used as the t-ERK1/2 Control for Figure 3.8 and Figure 3.19.

α-SMA and RAGE immunoreactive bands are also re-used in multiple figures; the immunoreactive band for the α-SMA Control sample shown in Figure 3.11 is also used as the α-SMA Control for Figure 3.12 and Figure 3.20. The immunoreactive band for the RAGE Control sample shown in Figure 3.13 is also used as the RAGE Control for Figure 3.1, Figure 3.2, Figure 3.3, Figure 3.10, Figure 3.14, Figure 3.15, Figure 3.17, and Figure 3.21.

Universal Control

After making 10% sodium dodecyl sulfate (SDS)-polyacrylamide gels, sample proteins including a universal control were loaded into the gel. The universal control was made up with equal amounts of fibroblast cells isolated from each of the untreated animals of the four Het groups. Use of universal control allowed for cross-comparison of Western blots.

Statistics

For basal fibroblast protein expression, unpaired student's T-test was performed using GraphPad Prism 5 software to test for statistical differences, defined as $p<0.05$. Error bars represent ± standard error of the mean (SEM).

CHAPTER III

RESULTS

The molecular mechanisms responsible for changes in fibroblast protein expression and phenotype switching during type II diabetes mellitus are not well understood. The purpose of this study was to identify a link between the PKA-dependent Rap1a signaling and the AGE-RAGE signaling cascade. The proposed studies determined if the downstream effects of AGE-RAGE signaling in type II diabetes mellitus are potentiated by the Rap1a GTPase via a PKA-dependent pathway. Changes to this signaling pathway would result in elevated outcomes including increased protein expression for α-smooth muscle actin, RAGE, and collagen, as well as PKA-dependent pathway signaling cascade markers, such as Rap1a, phospho-ERK1/2, and phospho-PKC-ζ.

Cardiac fibroblasts were isolated from genetically diabetic (db/db) and lean, heterozygous (Het) littermate mice, and a series of gain-of-function experiments were performed to test if the AGE-RAGE signaling cascades can operate in a Rap1a-PKA-dependent manner. In order to determine the effect of Rap1a-PKA-dependent signaling on the AGE-RAGE cascade, the AGE-RAGE pathway was blocked at the level of PKC-ζ using PKC-ζ pseudo-substrate. PKC-ζ is a key signaling hub in the AGE-RAGE signaling cascade, and it has been shown to be elevated when the cascade is activated[79].

In the figures of the following Results section, "Het Untreated" is used to distinguish from "Het" fibroblast cells. The "Het" cells were treated with either agonists or antagonists meaning these cells were treated.

Rap1a Results

Initial observations made by our laboratory suggested a possible role for Rap1a in the AGE-RAGE signaling cascade. Silencing Rap1a in diabetic (db/db) fibroblast returned diabetic levels of profibrotic markers to nondiabetic (Het Untreated) levels[83]. However, it was unclear where Rap1a intersected with the AGE-RAGE cascade. Results from this project aimed to identify where Rap1a intersected the AGE-RAGE cascade. In the first set of analysis, Rap1a protein expression was measured to determine changes in db/db and Het fibroblasts. As shown in Figure 3.1, Rap1a protein expression was found to be elevated in db/db fibroblasts and significantly increased in AGE stimulated fibroblasts as compared to Het Untreated fibroblasts. These changes returned to non-diabetic (Het Untreated) levels upon treatment with PKC-ζ pseudo-substrate.

For Specific Aim 1, isoproterenol (ISO) and 8-CPT-2Me-cAMP (EPAC Ag) treatment were used for a series of gain-of-function studies to increase Rap1a activity. In these experiments, Rap1a protein levels were found to be significantly elevated in both ISO and EPAC Ag treated db/db fibroblasts as shown in Figure 3.2 and Figure 3.3, respectively. Upon PKC-ζ Pseudo-substrate treatment, Rap1a expression was decreased to near non-diabetic (Het) levels despite AGE treatment (Figure 3.2 and Figure 3.3).

Collectively, the Rap1a results show that Rap1a protein levels in db/db fibroblasts were significantly elevated with both ISO and EPAC Ag treatments as compared to Rap1a protein levels in Het Untreated fibroblasts. However, upon PKC-ζ Pseudo-

substrate treatment, Rap1a protein levels in db/db fibroblasts was decreased to to near non-diabetic (Het Untreated) levels, regardless of the AGE treatment.

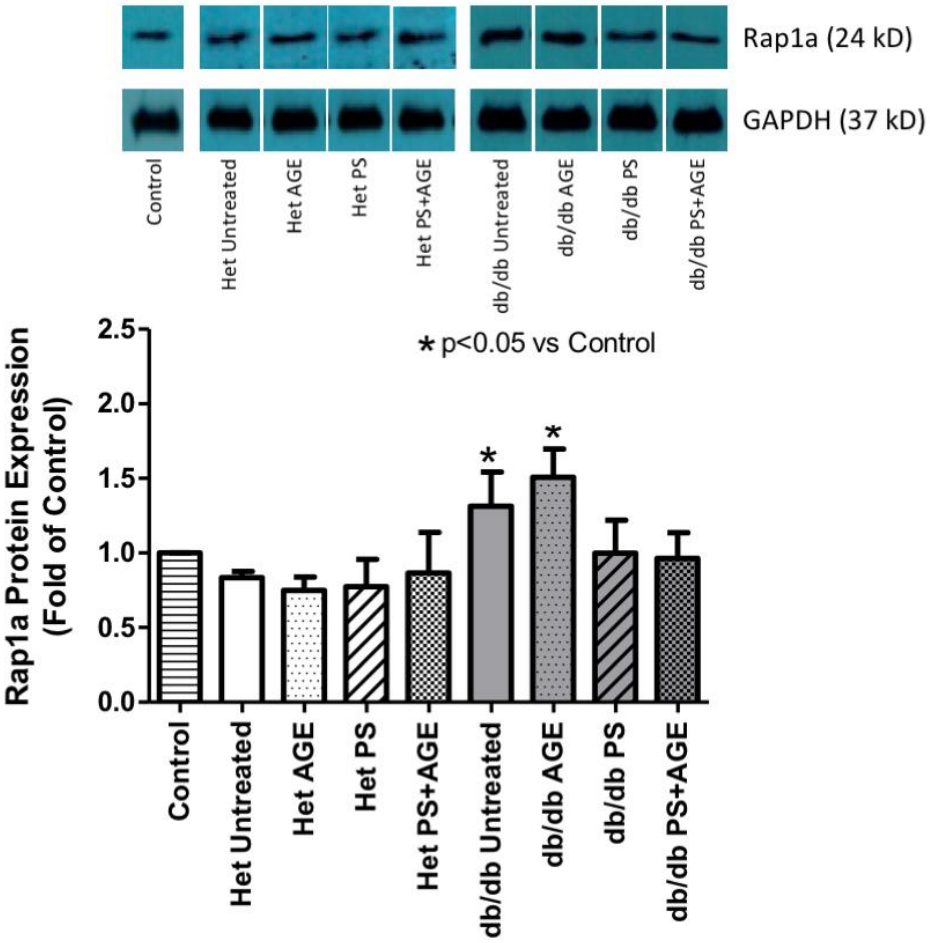

Figure 3.1 Fold change of Rap1a protein expression in Het and db/db isolated cardiac fibroblasts.

Rap1a protein expression was elevated in diabetic fibroblast and increased significantly in AGE stimulated cells. Rap1a protein expression levels were returned to non-diabetic levels (Het Untreated) upon treatment with PKC-ζ Pseudo-substrate (PS). "Het Untreated" is used to distinguish from "Het" cells; The "Het" cells shown in figures were treated with either agonists or antagonists. *$p<0.05$ vs. Control (universal control). Unless indicated, no significant differences were found when comparing similar treatment groups or within genotypic groups. Data represents an n-value of 4-6 separate isolations with 3-4 mice per isolation. Immunoreactive bands shown were taken from separate blots, for clarity, they are shown with the spaces between bands. Het and db/db sample groups were run on separate gels; however, the universal control was run on all gels and used to normalize across gels. The immunoreactive band for the Rap1a Control sample shown is also used as the Rap1a Control in Figure 3.2, Figure 3.3, and Figure 3.17. GAPDH immunoreactive bands shown are the same GAPDH immunoreactive bands as in Figure 3.10 and Figure 3.13. The immunoreactive band for the GAPDH Control sample shown is also used as the GAPDH Control for Figure 3.2, Figure 3.3, Figure 3.10, Figure 3.13, Figure 3.14, Figure 3.15, Figure 3.17, and Figure 3.21.

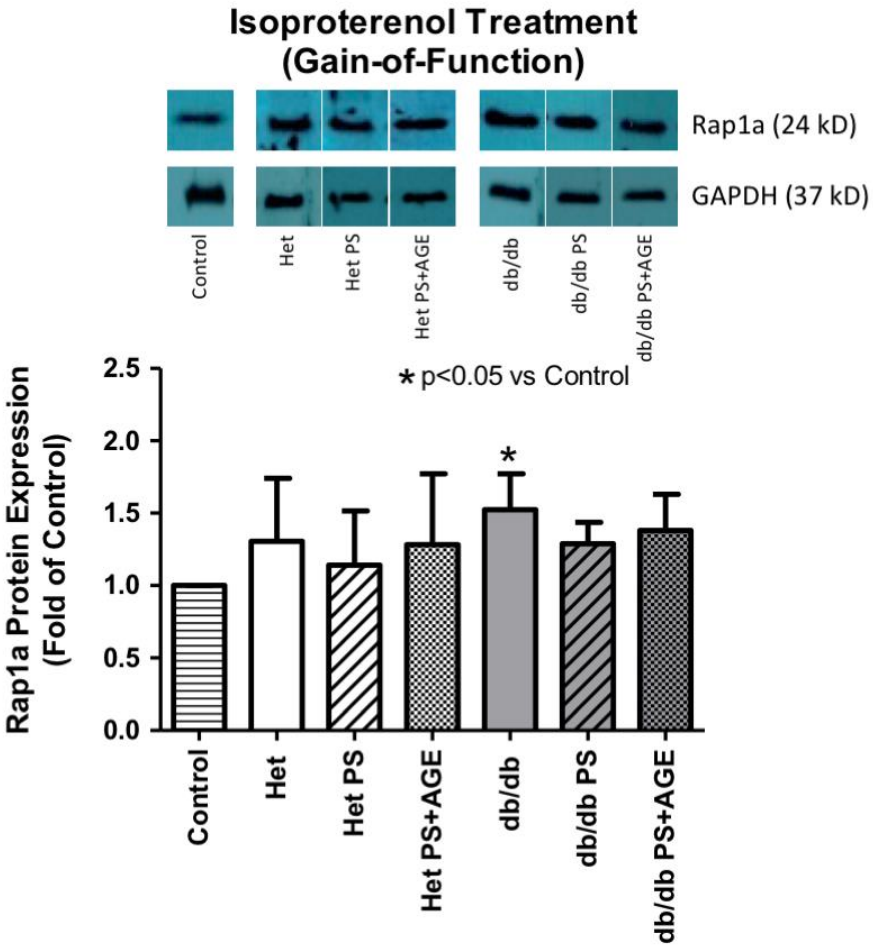

Figure 3.2 Fold change of Rap1a protein expression in Het and db/db isolated cardiac fibroblasts with Isoproterenol (ISO) treatment.

Rap1a protein expression levels were significantly elevated with ISO treatment in diabetic fibroblasts. Rap1a protein expression levels were returned to non-diabetic (Het Untreated) levels upon treatment with PKC-ζ Pseudo-substrate (PS). "Het Untreated" is used to distinguish from "Het" cells; The "Het" cells shown in figures were treated with either agonists or antagonists. *p<0.05 vs. Control (universal control). Unless indicated, no significant differences were found when comparing similar treatment groups or within genotypic groups. Data represents an n-value of 4-6 separate isolations with 3-4 mice per isolation. Immunoreactive bands shown were taken from separate blots, for clarity, they are shown with the spaces between bands. Het and db/db sample groups were run on separate gels; however, the universal control was run on all gels and used to normalize across gels. The immunoreactive band for the Rap1a Control sample shown is also used as the Rap1a Control in Figure 3.1, Figure 3.3, and Figure 3.17. GAPDH immunoreactive bands shown are the same GAPDH immunoreactive bands (except for GAPDH Control) as in Figure 3.11 and Figure 3.14. The immunoreactive band for the GAPDH Control sample shown is also used as the GAPDH Control for Figure 3.1, Figure 3.3, Figure 3.10, Figure 3.13, Figure 3.14, Figure 3.15, Figure 3.17, and Figure 3.21.

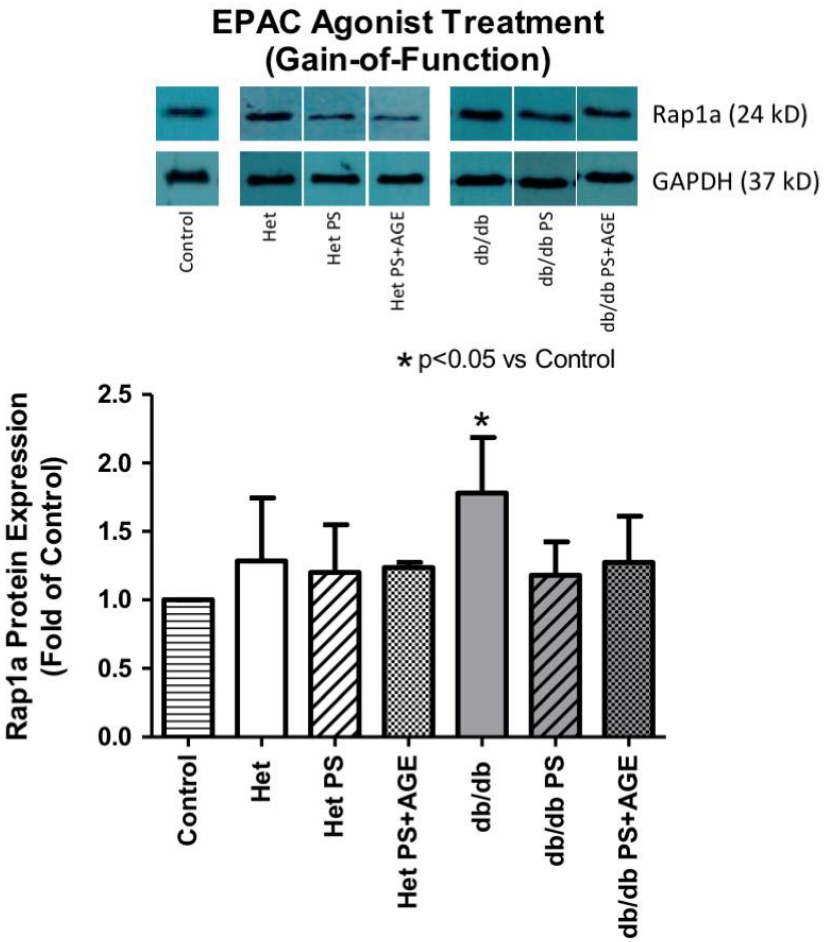

Figure 3.3 Fold change of Rap1a protein expression in Het and db/db isolated cardiac fibroblasts with 8-CPT-2Me-cAMP, an EPAC Agonist (EPAC Ag), treatment.

Rap1a protein expression levels were significantly elevated with EPAC Ag treatment in diabetic fibroblasts. Rap1a protein expression levels were returned to non-diabetic (Het Untreated) levels upon treatment with PKC-ζ Pseudo-substrate (PS). "Het Untreated" is used to distinguish from "Het" cells; The "Het" cells shown in figures were treated with either agonists or antagonists. *p<0.05 vs. Control (universal control). Unless indicated, no significant differences were found when comparing similar treatment groups or within genotypic groups. Data represents an n-value of 4-6 separate isolations with 3-4 mice per isolation. Immunoreactive bands shown were taken from separate blots, for clarity, they are shown with the spaces between bands. Het and db/db sample groups were run on separate gels; however, the universal control was run on all gels and used to normalize across gels. The immunoreactive band for the Rap1a Control sample shown is also used as the Rap1a Control in Figure 3.1, Figure 3.2, and Figure 3.17. GAPDH immunoreactive bands shown are the same GAPDH immunoreactive bands (except for GAPDH Control) as in Figure 3.12 and Figure 3.15. The immunoreactive band for the GAPDH Control sample shown is also used as the GAPDH Control for Figure 3.1, Figure 3.2, Figure 3.10, Figure 3.13, Figure 3.14, Figure 3.15, Figure 3.17, and Figure 3.21.

phospho-PKC-ζ Results

We wished to determine the protein expression levels of phospho-PKC-ζ (p-PKC-ζ) and total-PKC-ζ (t-PKC-ζ) as a result of AGE, PKC-ζ inhibition (PKC-ζ Pseudo-substrate), Isoproterenol (ISO), and 8-CPT-2Me-cAMP (EPAC Ag) treatments in non-diabetic (Het) and diabetic (db/db) fibroblasts. Our data agreed with previous studies in that p-PKC-ζ levels were significantly elevated in db/db fibroblasts treated with AGE to robustly stimulate RAGE as compared to the Het Untreated[32,51] (Figure 3.4). PKC-ζ inhibition returned phosphorylation levels to non-diabetic (Het) levels. Rap1a was then activated directly by 8-CPT-2Me-cAMP (EPAC Ag) or indirectly using Isoproterenol (ISO) to increase cAMP levels for gain-of-function experiments. Both ISO and EPAC Ag increased PKC-ζ phosphorylation in db/db fibroblasts. PKC-ζ inhibition returned phosphorylation levels back to non-diabetic (Het Untreated) levels (Figure 3.5 and Figure 3.6). Subsequent western blot analysis was performed to determine changes in ERK1/2 phosphorylation levels. ERK1/2 has been shown to function downstream from PKC-ζ, and ERK1/2 phosphorylation levels were elevated upon RAGE stimulation[79], shown in Figure 3.7.

Collectively, p-PKC-ζ levels were significantly elevated in db/db fibroblasts treated with AGE as compared to the Het Untreated fibroblasts treated with AGE; PKC-ζ Pseudo-substrate decreased the protein expression levels of db/db fibroblasts to non-diabetic (Het Untreated) levels despite the AGE treatment. ISO and EPAC Ag treatments increased p-PKC-ζ levels in db/db fibroblasts as compared to Het Untreated fibroblasts; PKC-ζ Pseudo-substrate decreased the protein expression levels of db/db fibroblasts to non-diabetic (Het Untreated) levels, despite the AGE treatment.

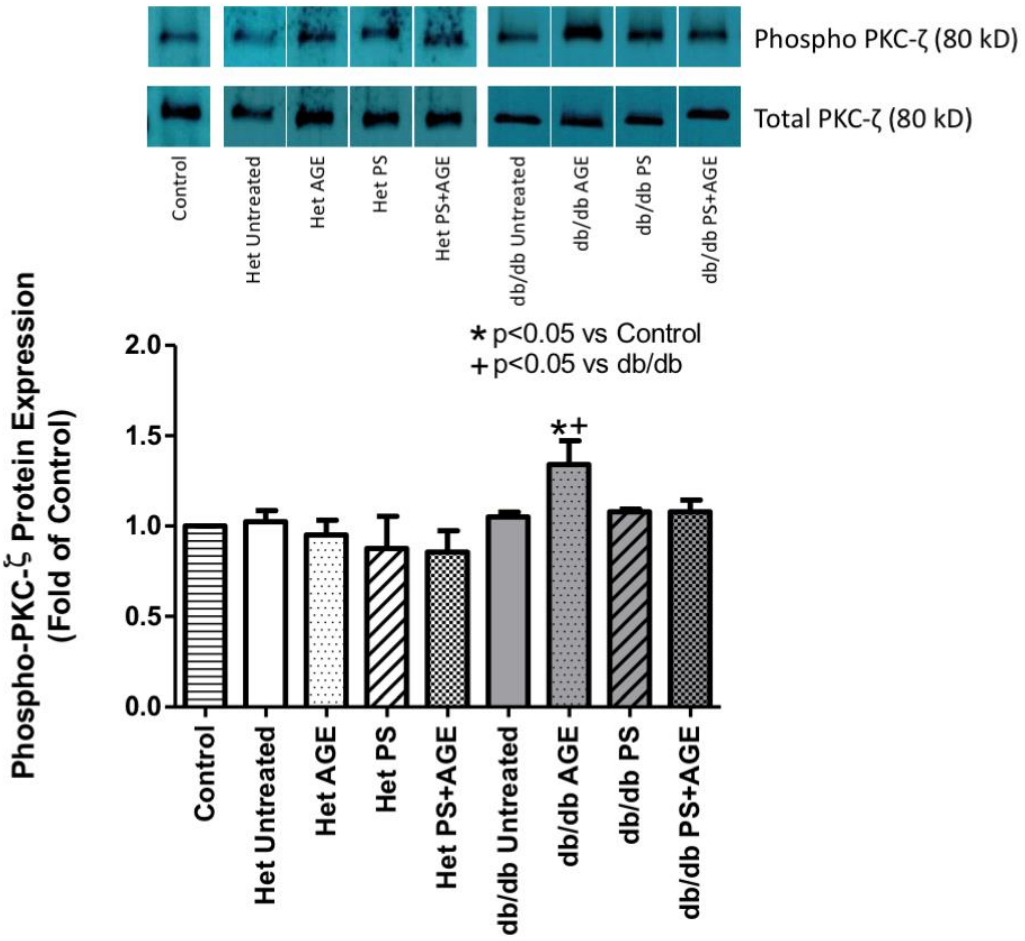

Figure 3.4 Fold change of phospho-PKC-ζ (p-PKC-ζ) protein expression in Het and db/db isolated cardiac fibroblasts.

p-PKC-ζ protein expression was significantly elevated in diabetic fibroblasts treated with AGE. p-PKC-ζ protein expression levels were returned to non-diabetic (Het Untreated) levels upon treatment with PKC-ζ Pseudo-substrate (PS). "Het Untreated" is used to distinguish from "Het" cells; The "Het" cells shown in figures were treated with either agonists or antagonists. *p<0.05 vs. Control (universal control); +p<0.05 vs. db/db (diabetic). Unless indicated, no significant differences were found when comparing similar treatment groups or within genotypic groups. Data represents an n-value of 4-6 separate isolations with 3-4 mice per isolation. Immunoreactive bands shown were taken from separate blots, for clarity, they are shown with the spaces between bands. Het and db/db sample groups were run on separate gels; however, the universal control was run on all gels and used to normalize across gels. The immunoreactive band for the p-PKC-ζ Control sample shown is also used as the p-PKC-ζ Control in Figure 3.5 and Figure 3.6. The immunoreactive band for the total-PKC-ζ (t-PKC-ζ) Control sample shown is also used as the t-PKC-ζ Control for Figure 3.5, Figure 3.6, and Figure 3.18.

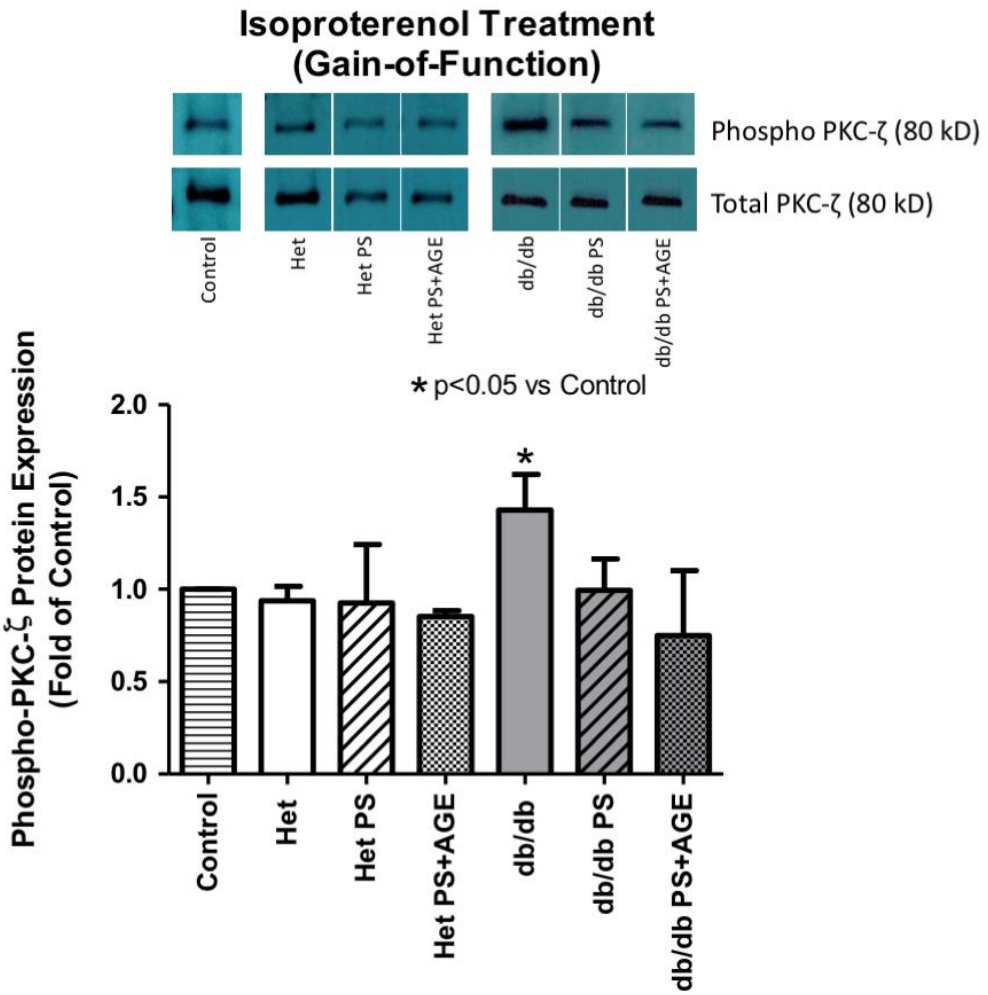

Figure 3.5 Fold change of phospho-PKC-ζ (p-PKC-ζ) protein expression in Het and db/db isolated cardiac fibroblasts with Isoproterenol (ISO) treatment.

p-PKC-ζ protein expression levels were significantly elevated with ISO treatment in diabetic fibroblasts. p-PKC-ζ protein expression levels were returned to non-diabetic (Het Untreated) levels upon treatment with PKC-ζ Pseudo-substrate (PS). "Het Untreated" is used to distinguish from "Het" cells; The "Het" cells shown in figures were treated with either agonists or antagonists. *p<0.05 vs. Control (universal control). Unless indicated, no significant differences were found when comparing similar treatment groups or within genotypic groups. Data represents an n-value of 4-6 separate isolations with 3-4 mice per isolation. Immunoreactive bands shown were taken from separate blots, for clarity, they are shown with the spaces between bands. Het and db/db sample groups were run on separate gels; however, the universal control was run on all gels and used to normalize across gels. The immunoreactive band for the p-PKC-ζ Control sample shown is also used as the p-PKC-ζ Control in Figure 3.4 and Figure 3.6. The immunoreactive band for the total-PKC-ζ (t-PKC-ζ) Control sample shown is also used as the t-PKC-ζ Control for Figure 3.4, Figure 3.6, and Figure 3.18.

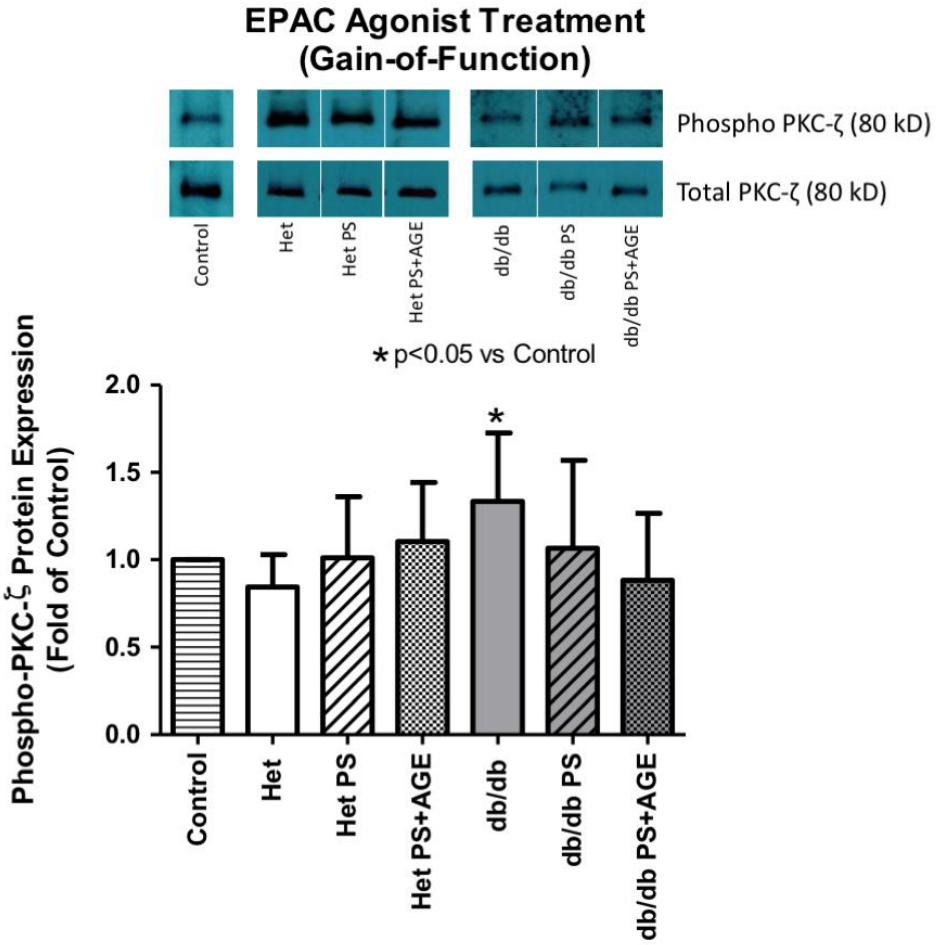

Figure 3.6 Fold change of phospho-PKC-ζ (p-PKC-ζ) protein expression in Het and db/db isolated cardiac fibroblasts with 8-CPT-2Me-cAMP, an EPAC Agonist (EPAC Ag), treatment.

p-PKC-ζ protein expression levels were significantly elevated with EPAC Ag treatment in diabetic fibroblasts. p-PKC-ζ protein expression levels were returned to non-diabetic (Het Untreated) levels upon treatment with PKC-ζ Pseudo-substrate (PS). "Het Untreated" is used to distinguish from "Het" cells; The "Het" cells shown in figures were treated with either agonists or antagonists. *p<0.05 vs. Control (universal control). Unless indicated, no significant differences were found when comparing similar treatment groups or within genotypic groups. Data represents an n-value of 4-6 separate isolations with 3-4 mice per isolation. Immunoreactive bands shown were taken from separate blots, for clarity, they are shown with the spaces between bands. Het and db/db sample groups were run on separate gels; however, the universal control was run on all gels and used to normalize across gels. The immunoreactive band for the p-PKC-ζ Control sample shown is also used as the p-PKC-ζ Control in Figure 3.4 and Figure 3.5. The immunoreactive band for the total-PKC-ζ (t-PKC-ζ) Control sample shown is also used as the t-PKC-ζ Control for Figure 3.4, Figure 3.5, and Figure 3.18.

phospho-ERK1/2 Results

In this study, phospho-ERK1/2 (p-ERK1/2) levels were also analyzed and were found to be significantly increased in AGE treated diabetic (db/db) fibroblasts as compared to non-diabetic (Het Untreated) fibroblasts. These results also complement the phospho-PKC-ζ results previously shown in Figure 3.4, in that, the AGE-RAGE signaling cascade is potentiated further downstream when the cascade is activated. Additionally, as before, there was a return to near normal (Het Untreated) levels in db/db fibroblasts treated with PKC-ζ Pseudo-substrate (Figure 3.7). With ISO and EPAC Ag, these data reflected similar findings as observed in phospho-PKC-ζ gain-of-function treatments that can be seen in Figure 3.8 and Figure 3.9, respectively.

Collectively, p-ERK1/2 levels were significantly elevated in db/db fibroblasts treated with AGE as compared to the Het Untreated fibroblasts treated with AGE; PKC-ζ Pseudo-substrate decreased the protein expression levels of db/db fibroblasts to non-diabetic (Het Untreated) levels despite the AGE treatment. ISO and EPAC Ag treatments increased p-ERK1/2 levels in db/db fibroblasts as compared to the Het Untreated fibroblasts; PKC-ζ Pseudo-substrate decreased the protein expression levels of db/db fibroblasts to non-diabetic (Het Untreated) levels, despite the AGE treatment.

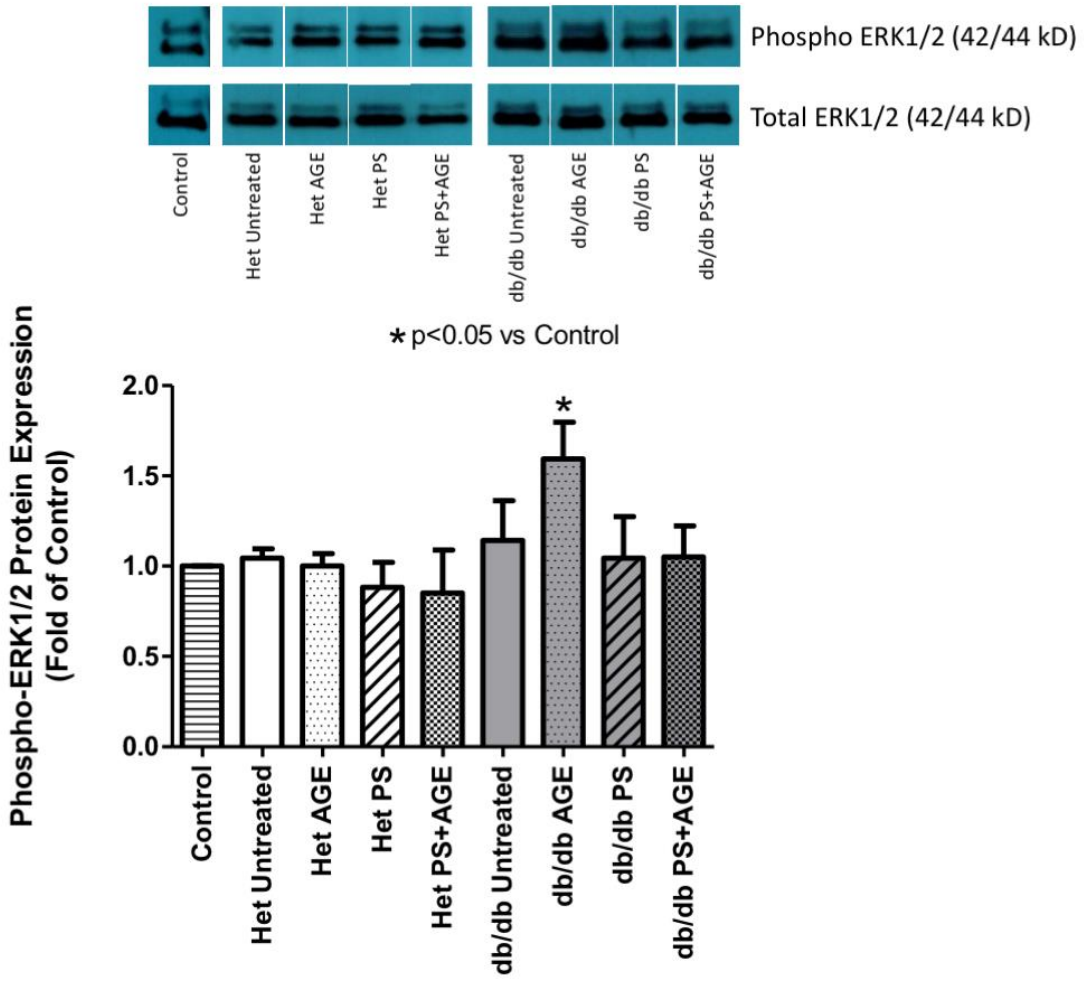

Figure 3.7 Fold change of phospho-ERK1/2 (p-ERK1/2) protein expression in Het and db/db isolated cardiac fibroblasts.

p-ERK1/2 protein expression was significantly elevated in diabetic fibroblasts treated with AGE. p-ERK1/2 protein expression levels were returned to non-diabetic (Het Untreated) levels upon treatment with PKC-ζ Pseudo-substrate (PS). "Het Untreated" is used to distinguish from "Het" cells; The "Het" cells shown in figures were treated with either agonists or antagonists. *p<0.05 vs. Control (universal control). Unless indicated, no significant differences were found when comparing similar treatment groups or within genotypic groups. Data represents an n-value of 4-6 separate isolations with 3-4 mice per isolation. Immunoreactive bands shown were taken from separate blots, for clarity, they are shown with the spaces between bands. Het and db/db sample groups were run on separate gels; however, the universal control was run on all gels and used to normalize across gels. The immunoreactive band for the p-ERK1/2 Control sample shown is also used as the p-ERK1/2 Control in Figure 3.8, Figure 3.9, and Figure 3.19. The immunoreactive band for the total-ERK1/2 (t-ERK1/2) Control sample shown is also used as the t-ERK1/2 Control for Figure 3.8, Figure 3.9, and Figure 3.19.

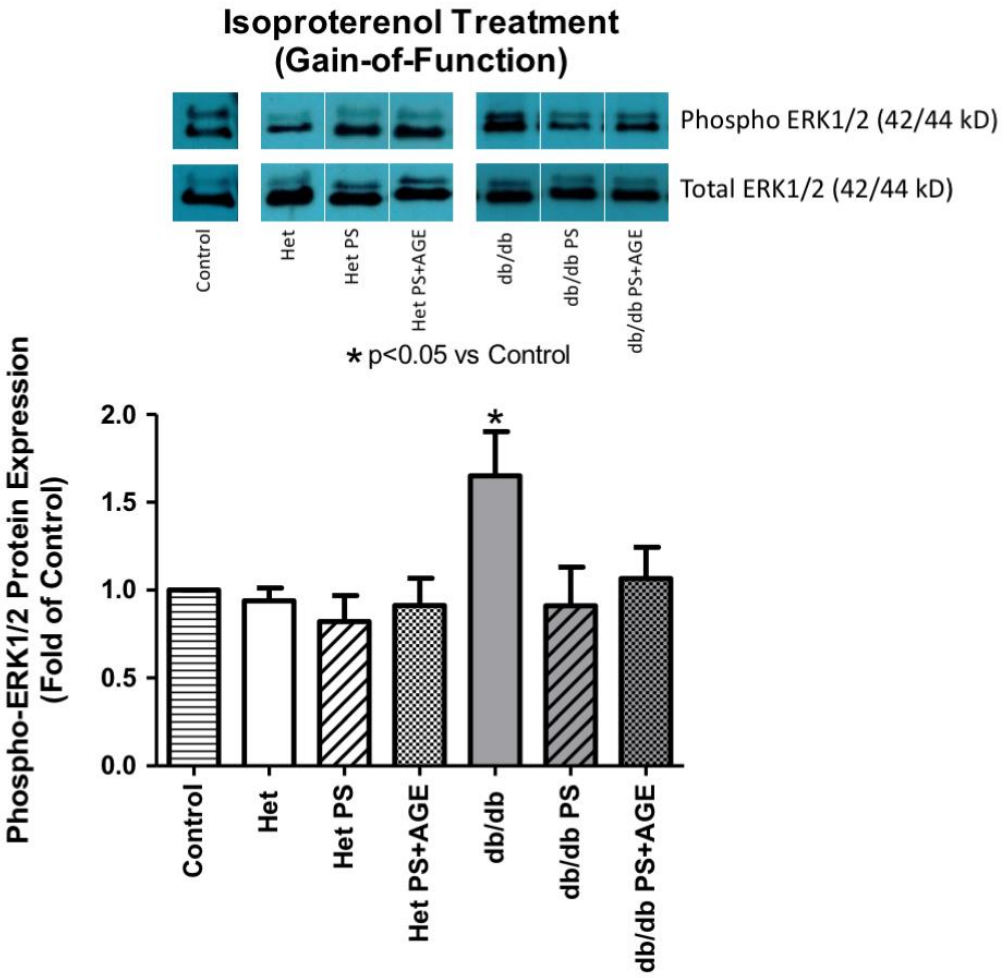

Figure 3.8 Fold change of phospho-ERK1/2 (p-ERK1/2) protein expression in Het and db/db isolated cardiac fibroblasts with Isoproterenol (ISO) treatment.

p-ERK1/2 protein expression levels were significantly elevated with ISO treatment in diabetic fibroblasts. p-ERK1/2 protein expression levels were returned to non-diabetic (Het Untreated) levels upon treatment with PKC-ζ Pseudo-substrate (PS). "Het Untreated" is used to distinguish from "Het" cells; The "Het" cells shown in figures were treated with either agonists or antagonists. *p<0.05 vs. Control (universal control). Unless indicated, no significant differences were found when comparing similar treatment groups or within genotypic groups. Data represents an n-value of 4-6 separate isolations with 3-4 mice per isolation. Immunoreactive bands shown were taken from separate blots, for clarity, they are shown with the spaces between bands. Het and db/db sample groups were run on separate gels; however, the universal control was run on all gels and used to normalize across gels. The immunoreactive band for the p-ERK1/2 Control sample shown is also used as the p-ERK1/2 Control in Figure 3.7, Figure 3.9, and Figure 3.19. The immunoreactive band for the total-ERK1/2 (t-ERK1/2) Control sample shown is also used as the t-ERK1/2 Control for Figure 3.7, Figure 3.9, and Figure 3.19.

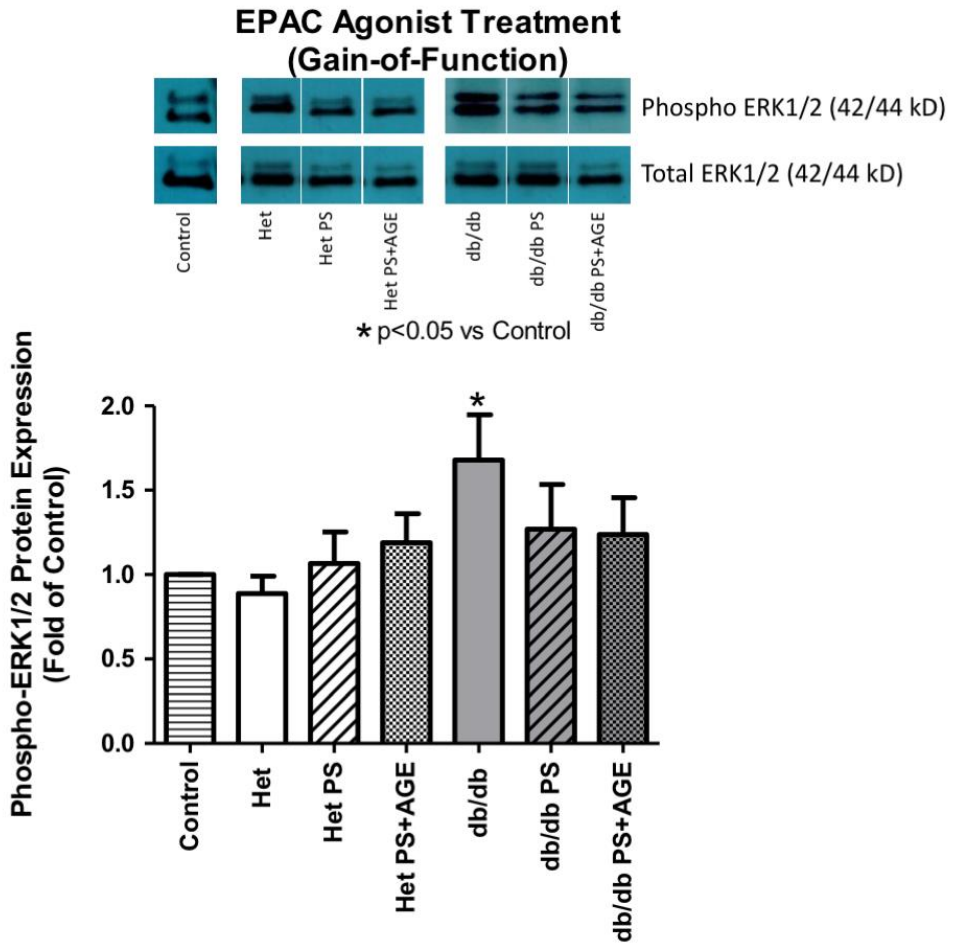

Figure 3.9 Fold change of phospho-ERK1/2 (p-ERK1/2) protein expression in Het and db/db isolated cardiac fibroblasts with 8-CPT-2Me-cAMP, an EPAC Agonist (EPAC Ag), treatment.

p-ERK1/2 protein expression levels were significantly elevated with EPAC Ag treatment in diabetic fibroblasts. p-ERK1/2 protein expression levels were returned to non-diabetic (Het Untreated) levels upon treatment with PKC-ζ Pseudo-substrate (PS). "Het Untreated" is used to distinguish from "Het" cells; The "Het" cells shown in figures were treated with either agonists or antagonists. *p<0.05 vs. Control (universal control). Unless indicated, no significant differences were found when comparing similar treatment groups or within genotypic groups. Data represents an n-value of 4-6 separate isolations with 3-4 mice per isolation. Immunoreactive bands shown were taken from separate blots, for clarity, they are shown with the spaces between bands. Het and db/db sample groups were run on separate gels; however, the universal control was run on all gels and used to normalize across gels. The immunoreactive band for the p-ERK1/2 Control sample shown is also used as the p-ERK1/2 Control in Figure 3.7, Figure 3.8, and Figure 3.19. The immunoreactive band for the total-ERK1/2 (t-ERK1/2) Control sample shown is also used as the t-ERK1/2 Control for Figure 3.7, Figure 3.8, and Figure 3.19.

α-SMA and RAGE Results

Increased phosphorylation levels of both PKC-ζ and ERK1/2 translated to elevated protein expression from several distinct downstream markers, such as α-smooth muscle actin (α-SMA) and RAGE. α-SMA and RAGE protein levels were quantitated by western blot analysis and were found to be significantly elevated in AGE treated db/db fibroblasts as compared to Het Untreated fibroblasts (Figure 3.10 and Figure 3.13, respectively). Administering agonists such as ISO and EPAC Ag for gain-of-function approaches complemented the phospho-PKC-ζ and phospho-ERK1/2 results as previously shown in Figure 3.5 and Figure 3.6 for phospho-PKC-ζ results and Figure 3.8 and Figure 3.9 for phospho-ERK1/2 results, respectively. In that, AGE-RAGE signaling cascade is potentiated further downstream resulting in a significant increase in protein expression of α-SMA (Figure 3.11 and Figure 3.12) and RAGE (Figure 3.14 and Figure 3.15).

Collectively, the α-SMA and RAGE protein levels were significantly elevated in AGE treated db/db fibroblasts as compared to Het Untreated fibroblasts. With both ISO and EPAC Ag treatments, protein levels in db/db fibroblasts were significantly elevated as compared to Het Untreated fibroblasts. However, upon PKC-ζ Pseudo-substrate treatment, α-SMA and RAGE protein levels in db/db fibroblasts was decreased to to near non-diabetic (Het Untreated) levels, regardless of the AGE treatment.

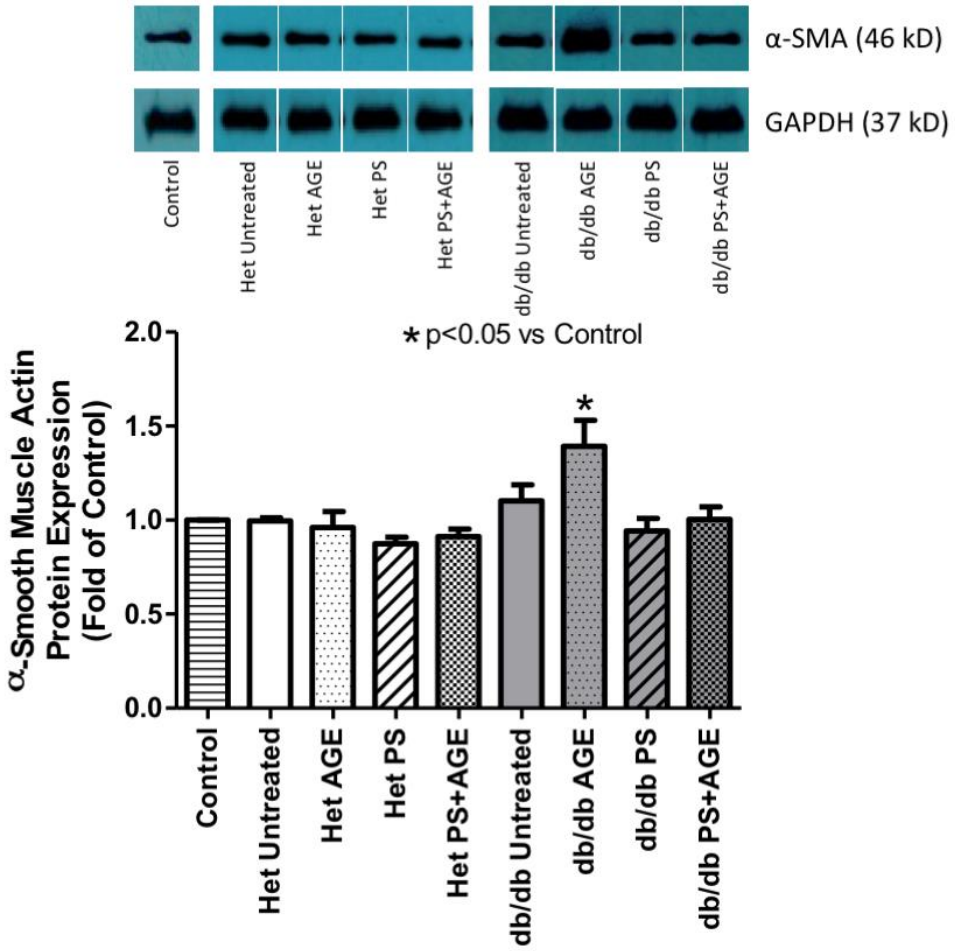

Figure 3.10 Fold change of α-Smooth Muscle Actin (α-SMA) protein expression in Het and db/db isolated cardiac fibroblasts.

α-SMA protein expression was significantly elevated in diabetic fibroblasts treated with AGE. α-SMA protein expression levels were returned to non-diabetic (Het Untreated) levels upon treatment with PKC-ζ Pseudo-substrate (PS). "Het Untreated" is used to distinguish from "Het" cells; The "Het" cells shown in figures were treated with either agonists or antagonists. *p<0.05 vs. Control (universal control). Unless indicated, no significant differences were found when comparing similar treatment groups or within genotypic groups. Data represents an n-value of 4-6 separate isolations with 3-4 mice per isolation. Immunoreactive bands shown were taken from separate blots, for clarity, they are shown with the spaces between bands. Het and db/db sample groups were run on separate gels; however, the universal control was run on all gels and used to normalize across gels. GAPDH immunoreactive bands shown are the same GAPDH immunoreactive bands as in Figure 3.1 and Figure 3.13. The immunoreactive band for the GAPDH Control sample shown is also used as the GAPDH Control for Figure 3.1, Figure 3.2, Figure 3.3, Figure 3.10, Figure 3.13, Figure 3.14, Figure 3.15, Figure 3.17, and Figure 3.21.

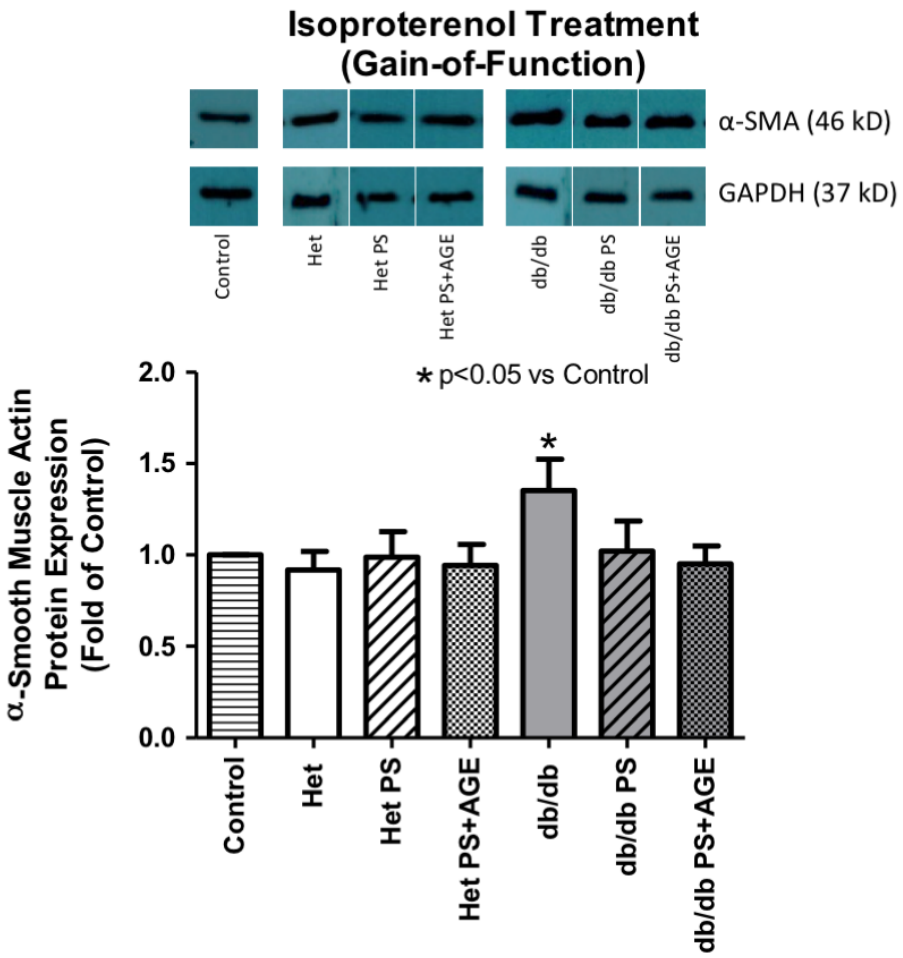

Figure 3.11 Fold change of α-Smooth Muscle Actin (α-SMA) protein expression in Het and db/db isolated cardiac fibroblasts with Isoproterenol (ISO) treatment.

α-SMA protein expression levels were significantly elevated with ISO treatment in diabetic fibroblasts. α-SMA protein expression levels were returned to non-diabetic (Het Untreated) levels upon treatment with PKC-ζ Pseudo-substrate (PS). "Het Untreated" is used to distinguish from "Het" cells; The "Het" cells shown in figures were treated with either agonists or antagonists. *p<0.05 vs. Control (universal control). Unless indicated, no significant differences were found when comparing similar treatment groups or within genotypic groups. Data represents an n-value of 4-6 separate isolations with 3-4 mice per isolation. Immunoreactive bands shown were taken from separate blots, for clarity, they are shown with the spaces between bands. Het and db/db sample groups were run on separate gels; however, the universal control was run on all gels and used to normalize across gels. The immunoreactive band for the α-SMA Control sample shown is also used as the α-SMA Control for Figure 3.12 and Figure 3.20. GAPDH immunoreactive bands shown are the same GAPDH immunoreactive bands (except for GAPDH Control) as in Figure 3.2 and Figure 3.14. The immunoreactive band for the GAPDH Control sample shown is also used as the GAPDH Control for Figure 3.12 and Figure 3.20.

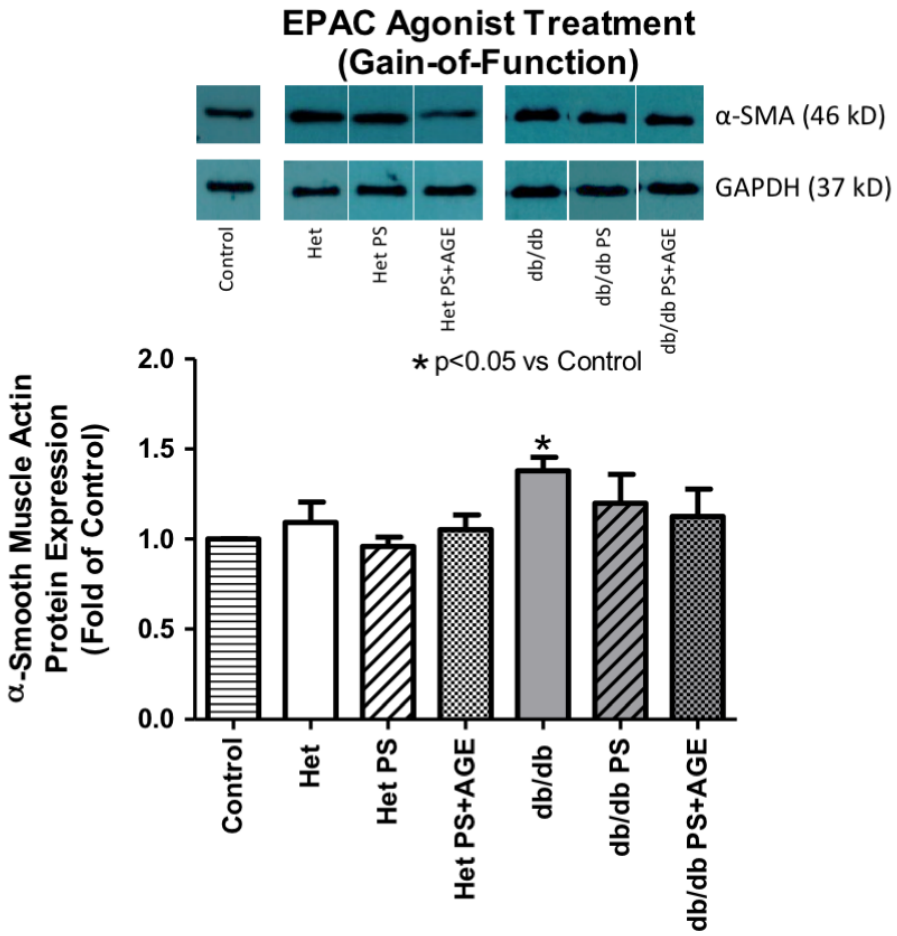

Figure 3.12 Fold change of α-Smooth Muscle Actin (α-SMA) protein expression in Het and db/db isolated cardiac fibroblasts with 8-CPT-2Me-cAMP, an EPAC Agonist (EPAC Ag), treatment.

α-SMA protein expression levels were significantly elevated with EPAC Ag treatment in diabetic fibroblasts. α-SMA protein expression levels were returned to non-diabetic (Het Untreated) levels upon treatment with PKC-ζ Pseudo-substrate (PS). "Het Untreated" is used to distinguish from "Het" cells; The "Het" cells shown in figures were treated with either agonists or antagonists. *p<0.05 vs. Control (universal control). Unless indicated, no significant differences were found when comparing similar treatment groups or within genotypic groups. Data represents an n-value of 4-6 separate isolations with 3-4 mice per isolation. Immunoreactive bands shown were taken from separate blots, for clarity, they are shown with the spaces between bands. Het and db/db sample groups were run on separate gels; however, the universal control was run on all gels and used to normalize across gels. The immunoreactive band for the α-SMA Control sample shown is also used as the α-SMA Control for Figure 3.11 and Figure 3.20. GAPDH immunoreactive bands shown are the same GAPDH immunoreactive bands (except for GAPDH Control) as in Figure 3.3 and Figure 3.15. The immunoreactive band for the GAPDH Control sample shown is also used as the GAPDH Control for Figure 3.11 and Figure 3.20.

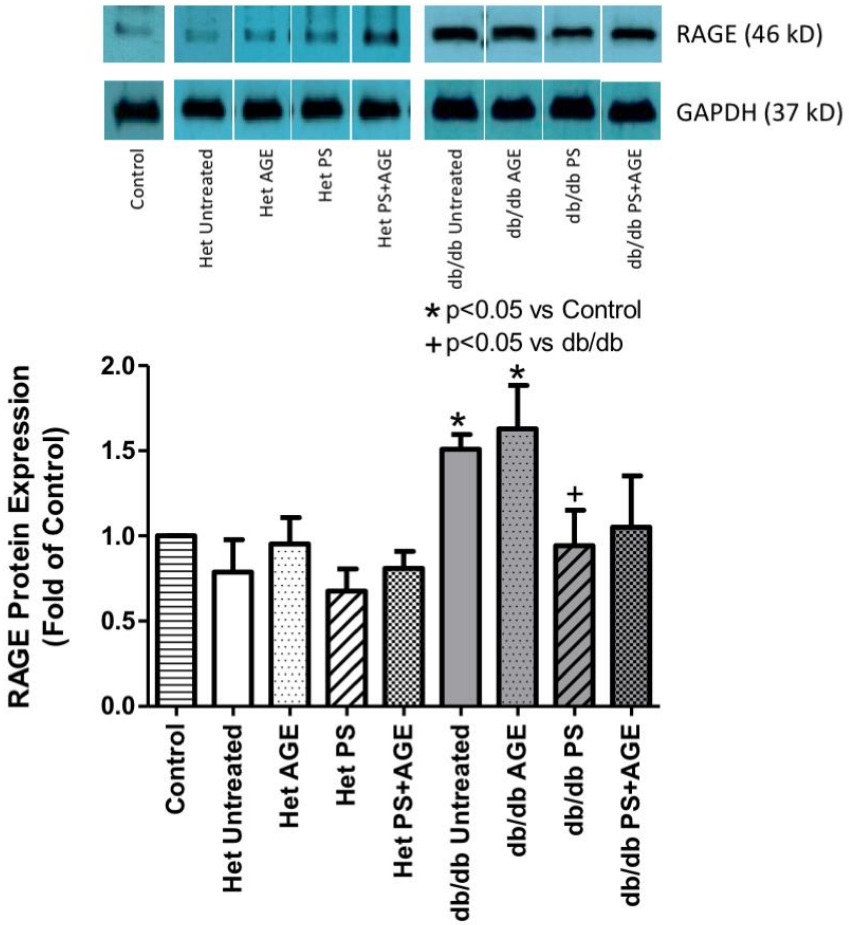

Figure 3.13 Fold change of RAGE protein expression in Het and db/db isolated cardiac fibroblasts.

RAGE protein expression was significantly elevated in diabetic fibroblasts treated with AGE. RAGE protein expression levels were returned to non-diabetic (Het Untreated) levels upon treatment with PKC-ζ Pseudo-substrate (PS). "Het Untreated" is used to distinguish from "Het" cells; The "Het" cells shown in figures were treated with either agonists or antagonists. *p<0.05 vs. Control (universal control). +p<0.05 vs. db/db (diabetic). Unless indicated, no significant differences were found when comparing similar treatment groups or within genotypic groups. Data represents an n-value of 4-6 separate isolations with 3-4 mice per isolation. Immunoreactive bands shown were taken from separate blots, for clarity, they are shown with the spaces between bands. Het and db/db sample groups were run on separate gels; however, the universal control was run on all gels and used to normalize across gels. The immunoreactive band for the RAGE Control sample shown is also used as the RAGE Control for Figure 3.14, Figure 3.15, Figure 3.21. GAPDH immunoreactive bands shown are the same GAPDH immunoreactive bands as in Figure 3.1 and Figure 3.10. The immunoreactive band for the GAPDH Control sample shown is also used as the GAPDH Control for Figure 3.1, Figure 3.2, Figure 3.3, Figure 3.10, Figure 3.14, Figure 3.15, Figure 3.17, and Figure 3.21.

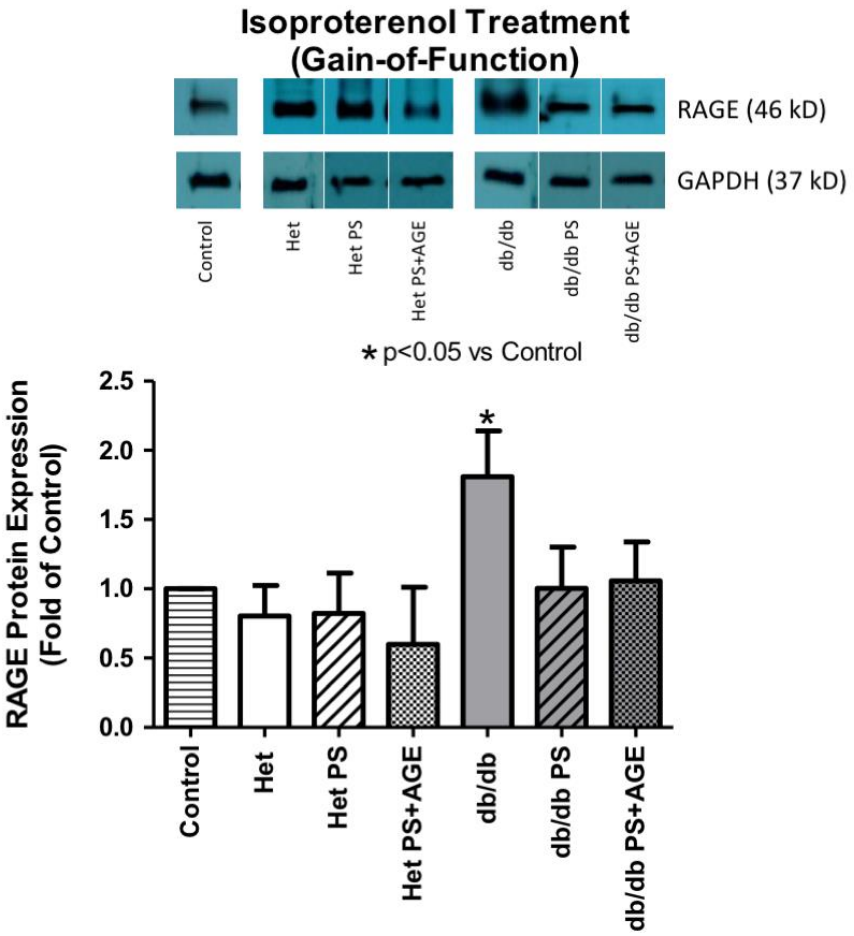

Figure 3.14 Fold change of RAGE protein expression in Het and db/db isolated cardiac fibroblasts with Isoproterenol (ISO) treatment.

RAGE protein expression levels were significantly elevated with ISO treatment in diabetic fibroblasts. RAGE protein expression levels were returned to non-diabetic (Het Untreated) levels upon treatment with PKC-ζ Pseudo-substrate (PS). "Het Untreated" is used to distinguish from "Het" cells; The "Het" cells shown in figures were treated with either agonists or antagonists. *p<0.05 vs. Control (universal control). Unless indicated, no significant differences were found when comparing similar treatment groups or within genotypic groups. Data represents an n-value of 4-6 separate isolations with 3-4 mice per isolation. Immunoreactive bands shown were taken from separate blots, for clarity, they are shown with the spaces between bands. Het and db/db sample groups were run on separate gels; however, the universal control was run on all gels and used to normalize across gels. The immunoreactive band for the RAGE Control sample shown is also used as the RAGE Control for Figure 3.13, Figure 3.15, Figure 3.21. GAPDH immunoreactive bands shown are the same GAPDH immunoreactive bands (except for GAPDH Control) as in Figure 3.2 and Figure 3.11. The immunoreactive band for the GAPDH Control sample shown is also used as the GAPDH Control for Figure 3.1, Figure 3.2, Figure 3.3, Figure 3.10, Figure 3.13, Figure 3.15, Figure 3.17, and Figure 3.21.

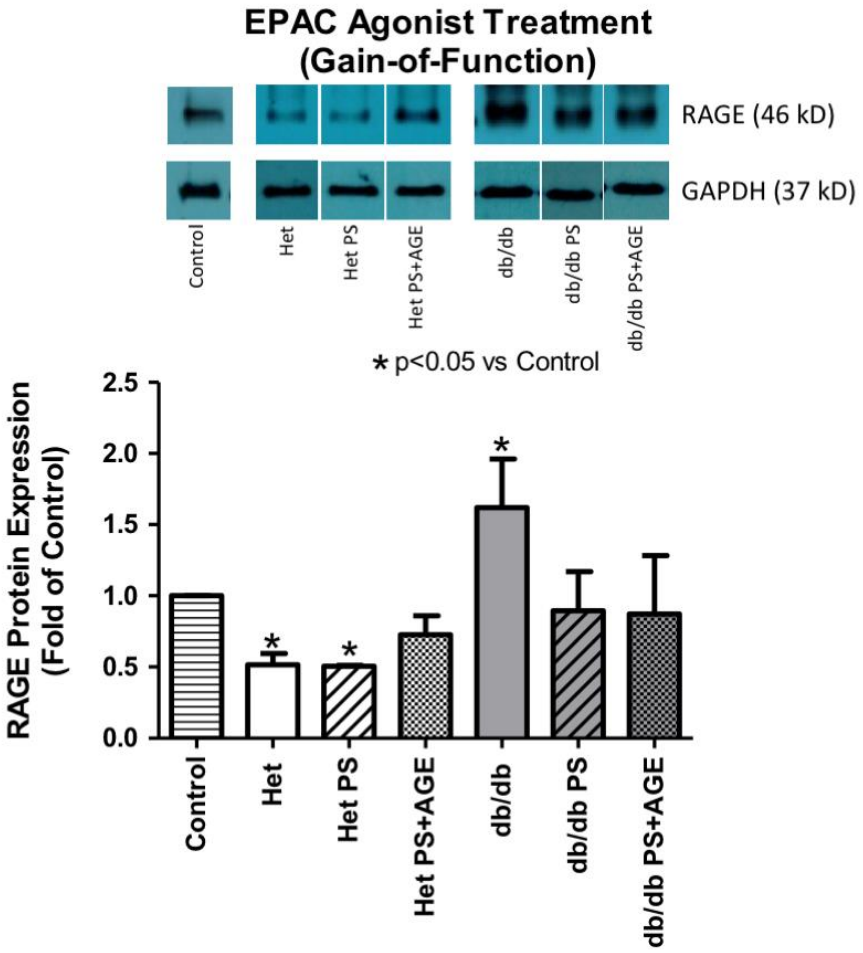

Figure 3.15 Fold change of RAGE protein expression in Het and db/db isolated cardiac fibroblasts with 8-CPT-2Me-cAMP, an EPAC Agonist (EPAC Ag), treatment.

RAGE protein expression levels were significantly elevated with EPAC Ag treatment in diabetic fibroblasts. RAGE protein expression levels were returned to non-diabetic (Het Untreated) levels upon treatment with PKC-ζ Pseudo-substrate (PS). "Het Untreated" is used to distinguish from "Het" cells; The "Het" cells shown in figures were treated with either agonists or antagonists. *p<0.05 vs. Control (universal control). Unless indicated, no significant differences were found when comparing similar treatment groups or within genotypic groups. Data represents an n-value of 4-6 separate isolations with 3-4 mice per isolation. Immunoreactive bands shown were taken from separate blots, for clarity, they are shown with the spaces between bands. Het and db/db sample groups were run on separate gels; however, the universal control was run on all gels and used to normalize across gels. The immunoreactive band for the RAGE Control sample shown is also used as the RAGE Control for Figure 3.13, Figure 3.14, Figure 3.21. GAPDH immunoreactive bands shown are the same GAPDH immunoreactive bands (except for GAPDH Control) as in Figure 3.3 and Figure 3.12. The immunoreactive band for the GAPDH Control sample shown is also used as the GAPDH Control for Figure 3.1, Figure 3.2, Figure 3.3, Figure 3.10, Figure 3.13, Figure 3.14, Figure 3.17, and Figure 3.21.

siRNA Rap1a Results

For Specific Aim 2, we used siRNA to downregulate the expression of Rap1a. In order to study the effect that a decrease in Rap1a would have on AGE/RAGE pathway we used siRNA to downregulate the expression of Rap1a. To confirm if Rap1a siRNA treatment worked successfully, a scramble siRNA treatment must be performed and compared to the siRNA Rap1a treatment data. Data from the scrambled siRNA is shown in Figure 3.16, which confirms my Rap1a siRNA treatment was successful. Quantified results are not provided due to our laboratory currently working on these studies. This scrambled siRNA treatment (Figure 3.16) was done by another lab member, Rushil Randive. Rap1a siRNA treatment of non-diabetic (Het) and diabetic (db/db) isolated cardiac fibroblasts significantly decreased Rap1a expression (Figure 3.16). Figure 3.17 shows the fold change of Rap1a protein expression in Het and db/db fibroblasts using Rap1a siRNA treatment. Downregulating Rap1a expression levels in diabetic fibroblasts translated into a restoration of signaling molecules, such as PKC-ζ and ERK1/2, to non-diabetic (Het Untreated) levels. In Figure 3.18, PKC-ζ phosphorylation levels in diabetic fibroblasts were returned to non-diabetic (Het Untreated) levels, however, in Figure 3.19, ERK1/2 phosphorylation was only slightly reduced. Despite the variable phospho-ERK1/2 levels in the fibroblasts, α-SMA and RAGE levels in diabetic fibroblasts were decreased to non-diabetic (Het Untreated) levels when Rap1a expression was downregulated (Figure 3.20 and Figure 3.21, respectively).

Collectively, the scrambled siRNA treatment showed no changes in Rap1a protein expression, unlike that of the Rap1a siRNA treatment, suggesting that the Rap1a siRNA treatment worked correctly. Downregulation of Rap1a expression levels in diabetic

fibroblasts translated into a restoration of signaling molecules, such as PKC-ζ, α-SMA, and RAGE protein levels, to non-diabetic (Het Untreated) levels; however, ERK1/2 was only slightly reduced.

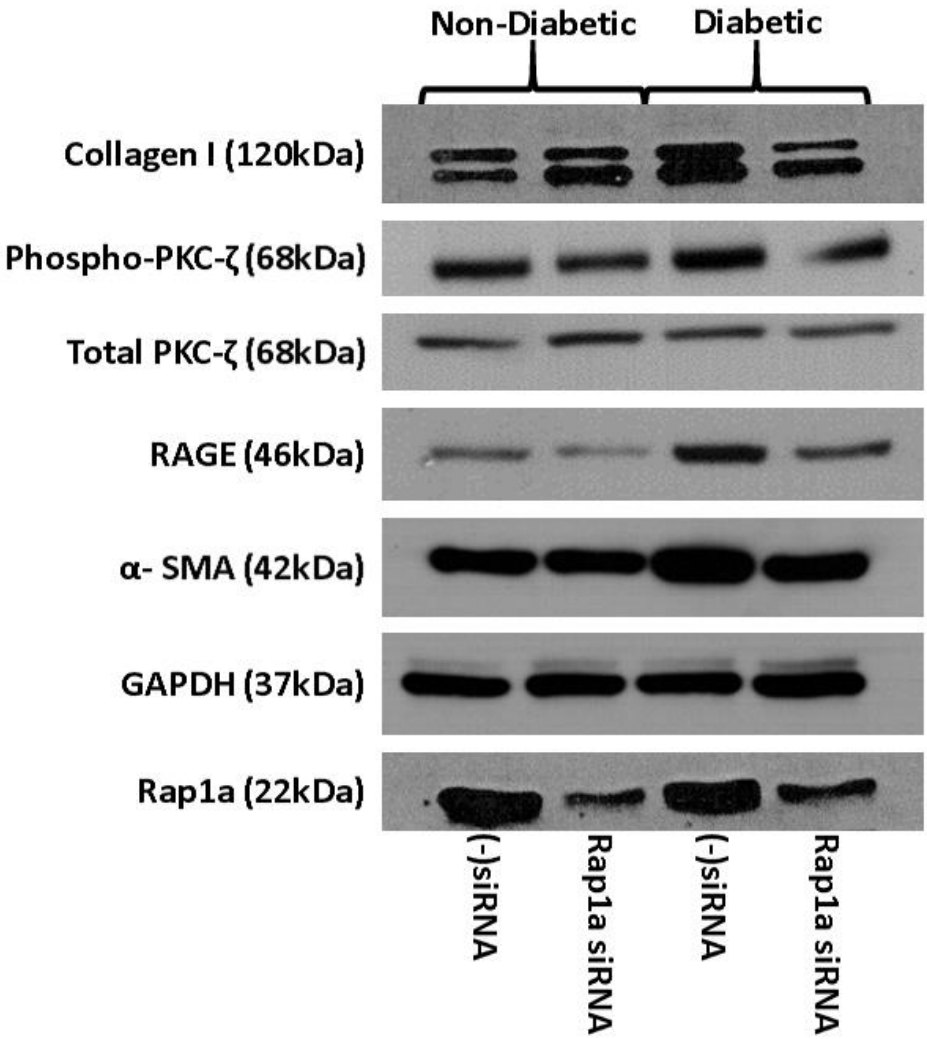

Figure 3.16 Qualitative representative protein expression in cells transfected with scrambled siRNA and Rap1a siRNA treatments in non-diabetic (Het) and diabetic (db/db) fibroblasts.

Scrambled siRNA [(-)siRNA] compared to Rap1a siRNA treatment in non-diabetic (Het) and diabetic (db/db) fibroblasts. (-)siRNA data shows no changes in protein expression like that of Rap1a siRNA, suggesting that Rap1a siRNA treatment worked correctly. Rap1a siRNA decreased Rap1a protein expression resulting in reduced expression of Collagen I, RAGE, α-SMA, and Rap1a in diabetic fibroblasts. GAPDH protein expression was not changed regardless of the treatments used. Changes in PKC-ζ expression was not clear. Data represent an n-value of 4-6 separate isolations with 3-4 mice per isolation. Quantified results are not provided due to our laboratory currently working on these studies.

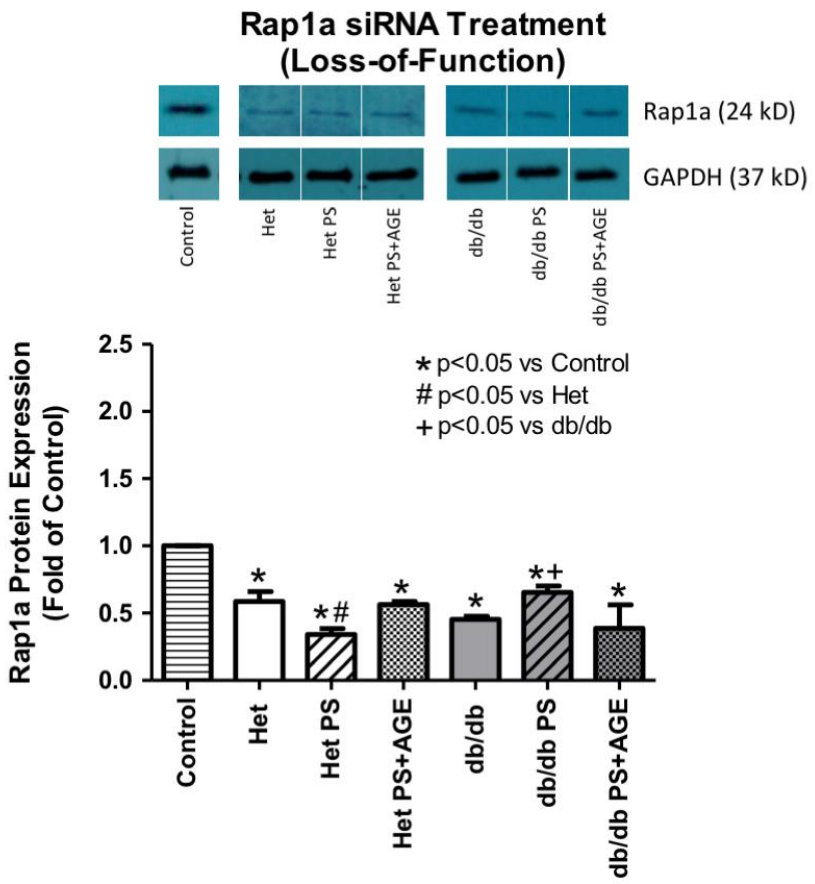

Figure 3.17 Fold change of Rap1a protein expression in Het and db/db isolated cardiac fibroblasts.

Rap1a siRNA treatment decreased AGE-RAGE signaling response in diabetic fibroblasts. Rap1a knockdown was equivalent to PKC-ζ Pseudo-substrate (PS) inhibition in Rap1a protein expression. "Het Untreated" is used to distinguish from "Het" cells; The "Het" cells shown in figures were treated with either agonists or antagonists. *p<0.05 vs. Control (universal control). #p<0.05 vs. Het (Het Untreated). +p<0.05 vs. db/db (diabetic). Unless indicated, no significant differences were found when comparing similar treatment groups or within genotypic groups. Data represents an n-value of 4-6 separate isolations with 3-4 mice per isolation. Immunoreactive bands shown were taken from separate blots, for clarity, they are shown with the spaces between bands. Het and db/db sample groups were run on separate gels; however, the universal control was run on all gels and used to normalize across gels. The immunoreactive band for the Rap1a Control sample shown is also used as the Rap1a Control in Figure 3.1, Figure 3.2, and Figure 3.3. The GAPDH immunoreactive bands shown are the same GAPDH immunoreactive bands as in Figure 3.20 and Figure 3.21. The immunoreactive band for the GAPDH Control sample shown is also used as the GAPDH Control for Figure 3.1, Figure 3.2, Figure 3.3, Figure 3.10, Figure 3.13, Figure 3.14, Figure 3.15, and Figure 3.21.

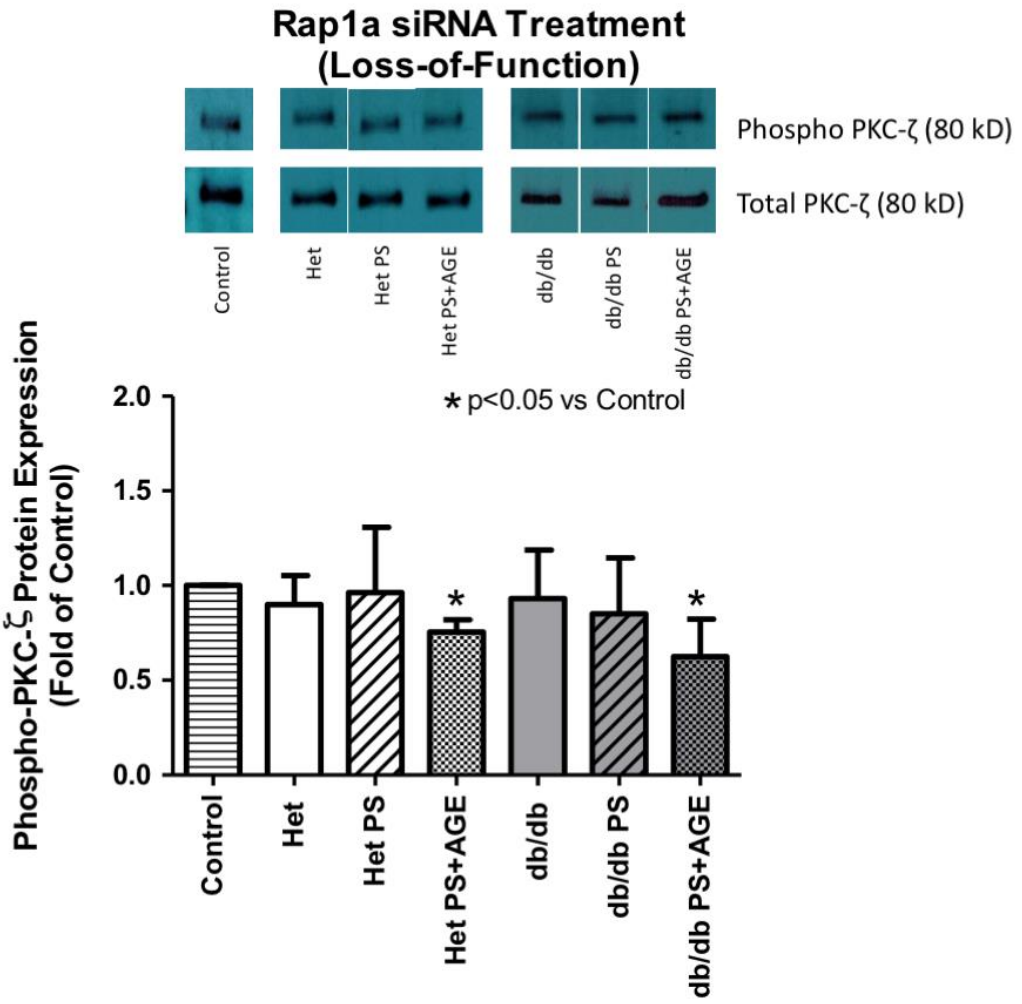

Figure 3.18 Fold change of phospho-PKC-ζ (p-PKC-ζ) protein expression in Het and db/db fibroblasts with Rap1a siRNA treatment in isolated cardiac fibroblasts.

Rap1a siRNA treatment decreased AGE-RAGE signaling response in diabetic fibroblasts. Rap1a knockdown was equivalent to PKC-ζ Pseudo-substrate (PS) inhibition in PKC-ζ protein expression. "Het Untreated" is used to distinguish from "Het" cells; The "Het" cells shown in figures were treated with either agonists or antagonists. *p<0.05 vs. Control (universal control). Unless indicated, no significant differences were found when comparing similar treatment groups or within genotypic groups. Data represents an n-value of 4-6 separate isolations with 3-4 mice per isolation. Immunoreactive bands shown were taken from separate blots, for clarity, they are shown with the spaces between bands. Het and db/db sample groups were run on separate gels; however, the universal control was run on all gels and used to normalize across gels. The immunoreactive band for the total-PKC-ζ (t-PKC-ζ) Control sample shown is also used as the t-PKC-ζ Control for Figure 3.5, Figure 3.6, and Figure 3.18.

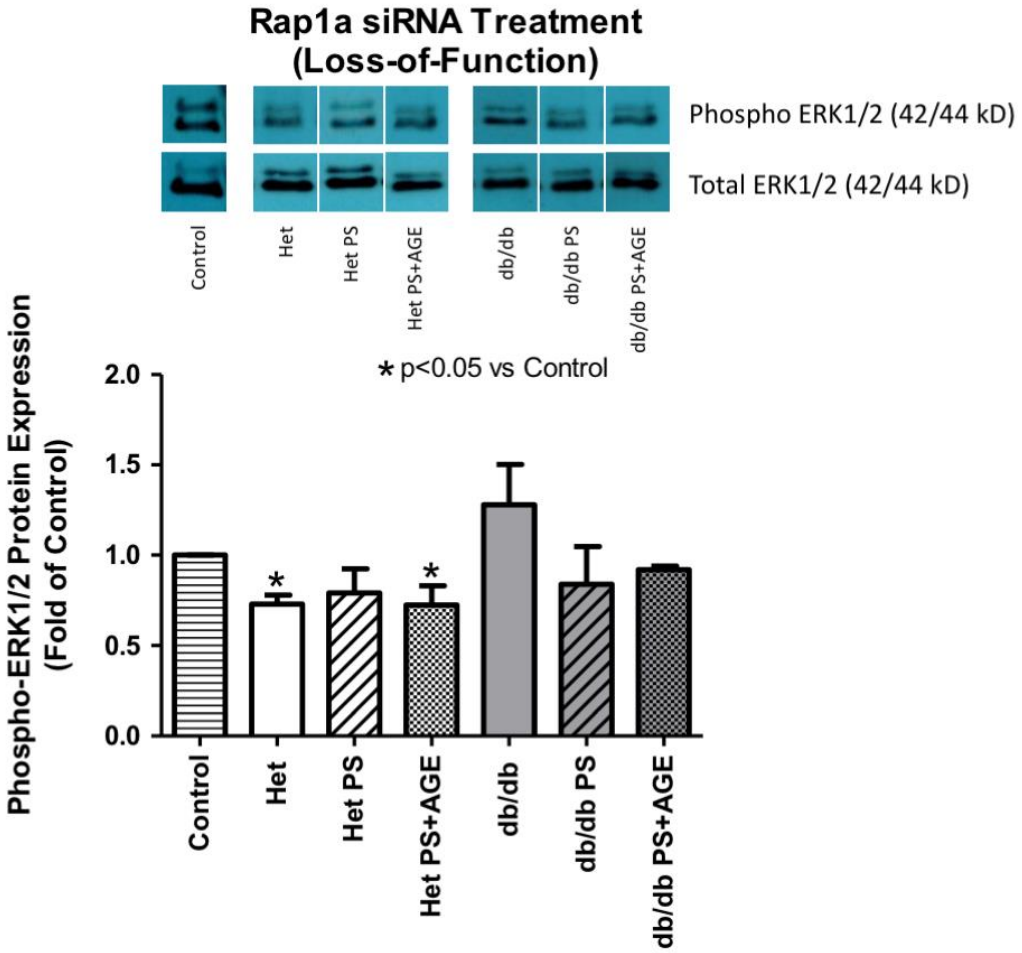

Figure 3.19 Fold change of phospho-ERK1/2 (p-ERK1/2) protein expression in Het and db/db fibroblasts with Rap1a siRNA treatment in isolated cardiac fibroblasts.

Rap1a siRNA treatment decreased AGE-RAGE signaling response in diabetic fibroblasts. Rap1a knockdown did not downregulate p-ERK1/2 protein expression compared to PKC-ζ Pseudo-substrate (PS) inhibition. "Het Untreated" is used to distinguish from "Het" cells; The "Het" cells shown in figures were treated with either agonists or antagonists. *p<0.05 vs. Control (universal control). Unless indicated, no significant differences were found when comparing similar treatment groups or within genotypic groups. Data represents an n-value of 4-6 separate isolations with 3-4 mice per isolation. Immunoreactive bands shown were taken from separate blots, for clarity, they are shown with the spaces between bands. Het and db/db sample groups were run on separate gels; however, the universal control was run on all gels and used to normalize across gels. The immunoreactive band for the p-ERK1/2 Control sample shown is also used as the p-ERK1/2 Control in Figure 3.7, Figure 3.8, and Figure 3.9. The immunoreactive band for the total-ERK1/2 (t-ERK1/2) Control sample shown is also used as the t-ERK1/2 Control for Figure 3.7, Figure 3.8, and Figure 3.9.

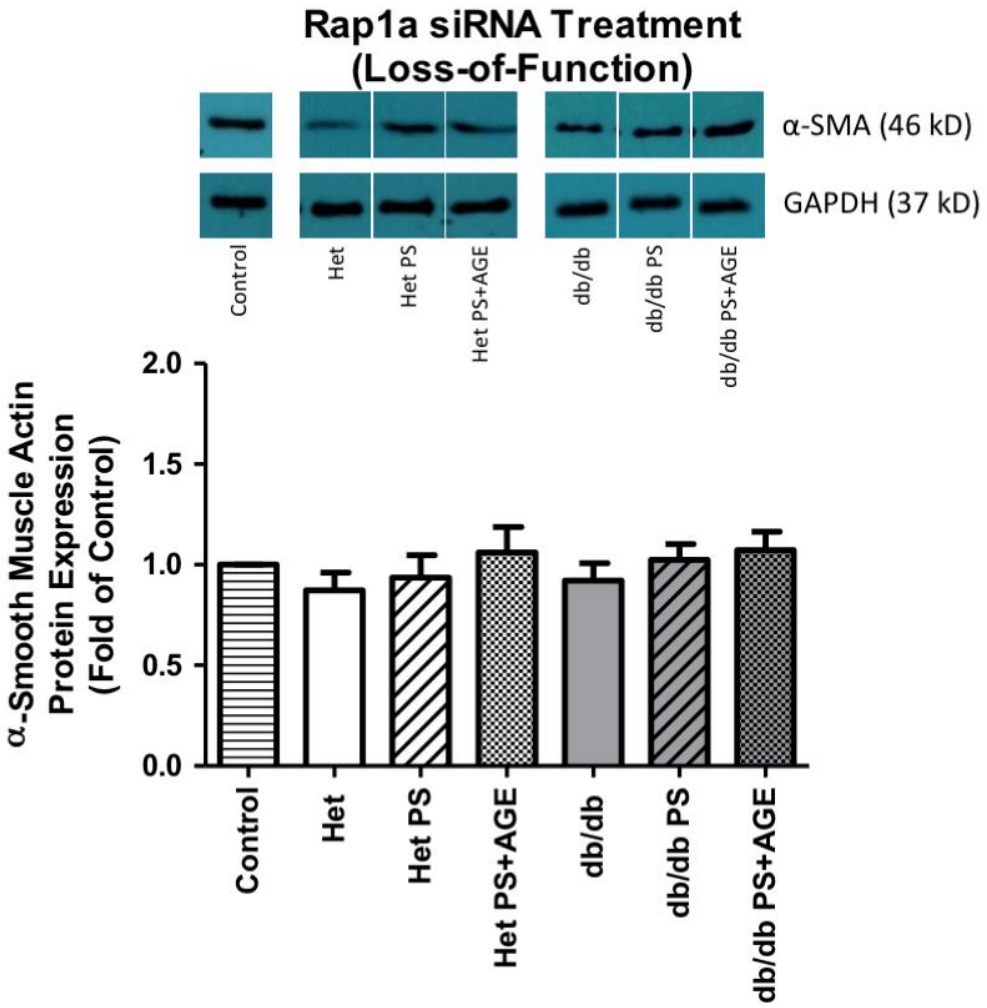

Figure 3.20 Fold change of α-Smooth Muscle Actin (α-SMA) protein expression in Het and db/db isolated cardiac fibroblasts.

Rap1a siRNA treatment decreased AGE-RAGE signaling response in diabetic fibroblasts. Rap1a knockdown was equivalent to PKC-ζ Pseudo-substrate (PS) inhibition in α-SMA protein expression. "Het Untreated" is used to distinguish from "Het" cells; The "Het" cells shown in figures were treated with either agonists or antagonists. Unless indicated, no significant differences were found when comparing similar treatment groups or within genotypic groups. Data represents an n-value of 4-6 separate isolations with 3-4 mice per isolation. Immunoreactive bands shown were taken from separate blots, for clarity, they are shown with the spaces between bands. Het and db/db sample groups were run on separate gels; however, the universal control was run on all gels and used to normalize across gels. The immunoreactive band for the α-SMA Control sample shown is also used as the α-SMA Control for Figure 3.11 and Figure 3.12. GAPDH immunoreactive bands shown are the same GAPDH immunoreactive bands as in Figure 3.17 and Figure 3.21. The immunoreactive band for the GAPDH Control sample shown is also used as the GAPDH Control for Figure 3.11 and Figure 3.12.

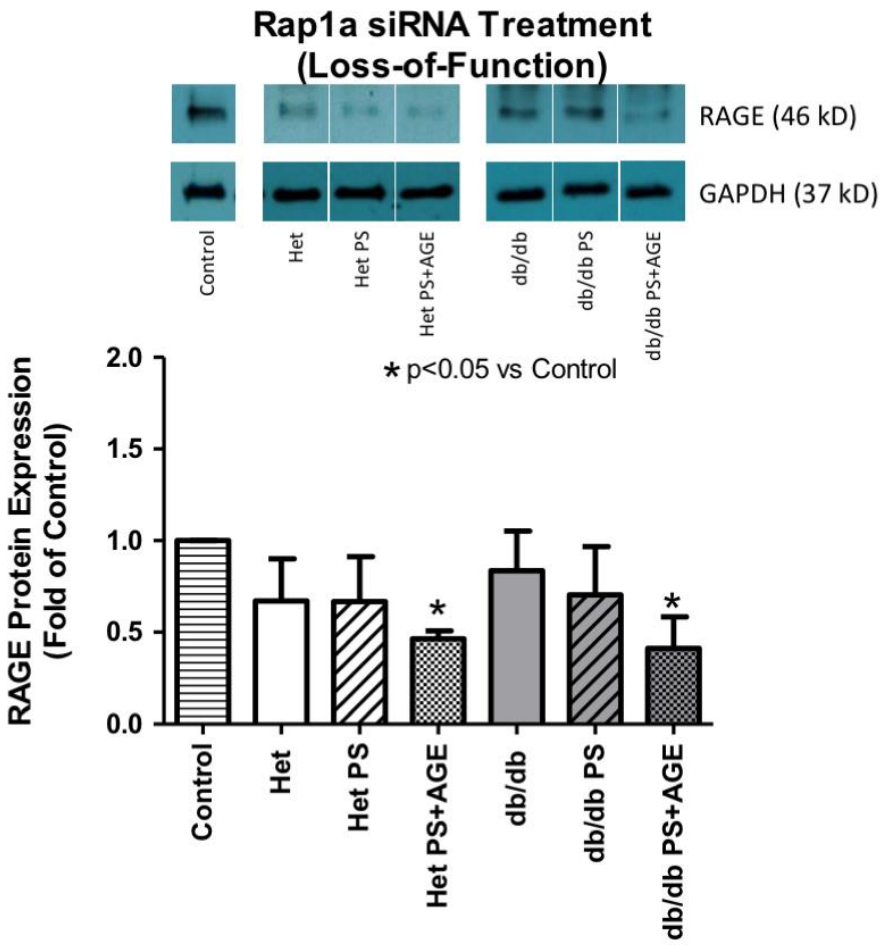

Figure 3.21 Fold change of RAGE protein expression in Het and db/db isolated cardiac fibroblasts.

Rap1a siRNA treatment decreased AGE-RAGE signaling response in diabetic fibroblasts. Rap1a knockdown was equivalent to PKC-ζ Pseudo-substrate (PS) inhibition in RAGE protein expression. "Het Untreated" is used to distinguish from "Het" cells; The "Het" cells shown in figures were treated with either agonists or antagonists. *$p<0.05$ vs. Control (universal control). Unless indicated, no significant differences were found when comparing similar treatment groups or within genotypic groups. Data represents an n-value of 4-6 separate isolations with 3-4 mice per isolation. Immunoreactive bands shown were taken from separate blots, for clarity, they are shown with the spaces between bands. Het and db/db sample groups were run on separate gels; however, the universal control was run on all gels and used to normalize across gels. The immunoreactive band for the RAGE Control sample shown is also used as the RAGE Control for Figure 3.13, Figure 3.14, Figure 3.15. GAPDH immunoreactive bands shown in Figure 3.17 are the same GAPDH immunoreactive bands as in Figure 3.17 and Figure 3.20. The immunoreactive band for the GAPDH Control sample shown is also used as the GAPDH Control for Figure 3.1, Figure 3.2, Figure 3.3, Figure 3.10, Figure 3.13, Figure 3.14, Figure 3.15, and Figure 3.17.

The presented data demonstrates a link exists between Rap1a and the AGE-RAGE signaling cascade. The performed studies determined that the downstream effects of AGE-RAGE signaling in diabetes II mellitus is potentiated by Rap1a. Changes in Rap1a expression through either gain-of-function or loss-of-function experiments resulted in comparable alterations in protein expression in defined AGE-RAGE cascade outcomes, such as α-SMA and RAGE. In addition, AGE-RAGE signal transduction molecules, such as PKC- ζ and ERK1/2, had similar phosphorylation responses upon Rap1a stimulation or Rap1a downregulation. Inhibiting PKC-ζ phosphorylation by administering PKC-ζ pseudo-substrate *in vitro* halted downstream progression of the Rap1a-AGE-RAGE signaling cascade. Thus, from this data we have determined that Rap1a exerts its effects on the AGE-RAGE cascade through crosstalk with PKC-ζ. While further confirmation studies need to be performed, these studies are the first of its kind to provide Rap1a as a unique target for therapeutic strategies aimed at reducing chronic hyperglycemia-mediated ECM production and accumulation in diabetic patients.

CHAPTER IV

DISCUSSION

The purpose of this study was to identify a role for PKA-dependent Rap1a signaling in the AGE-RAGE cascade. We hypothesized that Rap1a, via a PKA-dependent pathway, increases the downstream effects of AGE-RAGE signaling in type II diabetes mellitus leading to elevated ECM accumulation and remodeling in the heart. In order in to test this hypothesis, two specific aims were proposed. Specific Aim 1 was to define a link between PKA and the AGE-RAGE signaling cascade, *in vitro*. We hypothesized that the AGE-RAGE signaling cascade operates in a PKA-dependent manner to activate Rap1a to stimulate downstream modulators. In Specific Aim 2, our focus was to determine if changes in Rap1a GTPase and/or expression altered PKA directed changes in AGE-RAGE signaling, *in vitro*.

In Specific Aim 1, it was found that Rap1a expression was increased in diabetic fibroblasts as compared to the heterozygous fibroblasts, *in vitro*. Gain-of-function studies were performed to stimulate two different upstream modulators of Rap1a; both ISO and EPAC Ag increased Rap1a protein levels to mediated changes in AGE-RAGE signaling. Increased phosphorylation of signaling markers, such as ERK1/2 and PKC- ζ, led to elevated α-SMA and RAGE protein levels. In order to understand where Rap1a fits into the AGE-RAGE cascade and how changes in Rap1a activity might affect AGE-RAGE-mediated outcomes, we inhibited PKC-ζ phosphorylation using PKC-ζ Pseudo-substrate

(PS). These inhibitory studies focused on PKC-ζ as one the known signaling hubs in the AGE-RAGE cascade[79]. Thus, allowing us to determine whether Rap1a-mediated AGE-RAGE cascade integration occurs upstream or downstream of PKC-ζ. The presented data demonstrated that PKC-ζ inhibition in db/db fibroblasts returned phospho-PKC-ζ, Figure 3.5 and 3.6, and phospho-ERK1/2, Figure 3.8 and Figure 3.9, to non-diabetic levels. PKC-ζ inhibition interrupted ISO and EPAC Ag-mediated Rap1a stimulation of the AGE-RAGE signaling. Therefore, changes observed were due to elevated Rap1a crosstalk with PKC-ζ in the AGE-RAGE cascade (Figure 3.1). In this study, we have defined a link between Rap1a and AGE-RAGE signaling cascades. We have successfully shown that activating Rap1a will result in stimulating downstream mediators, such as PKC-ζ and ERK1/2, to increase protein expression of known outcomes of the AGE-RAGE signaling cascade.

In Specific Aim 2, it was found that changes in Rap1a GTPase expression affected PKA-dependent AGE-RAGE signaling, *in vitro*. Loss-of-function studies using Rap1a siRNA treatment potentially showed that Rap1a could be a key mediator in PKA-dependent AGE-RAGE signaling. Downregulation of Rap1a expression decreased ISO and EPAC Ag stimulation of the AGE-RAGE signaling. PKC-ζ and ERK1/2 phosphorylation should have also been decreased as a result of Rap1a protein downregulation. PKC-ζ phosphorylation levels in diabetic fibroblasts returned to non-diabetic levels which can be seen in Figure 3.18. However, it can be observed in Figure 3.19, ERK1/2 phosphorylation was only slightly reduced. For these studies, we are uncertain as to why there was not a more significant, less variable (such as the results of PKC-ζ) response in ERK1/2 phosphorylation levels.

There are a number of plausible explanations regarding ERK1/2 response. Some possible explanations may be that a number of other signaling cascades converge at ERK1/2 to cause increased phosphorylation[14]. Additionally, ERK1/2 phosphorylation levels have been demonstrated to fluctuate and rapidly cycle due to mechanical and sheer stresses on the cells[38]. Therefore, changes in phospho-ERK1/2 can be a result of handling or processing samples for protein harvesting. One may argue that there was a downregulation in protein expression of PKC-ζ, α-SMA, and RAGE due to PKC-ζ PS not Rap1a siRNA; however, even without PKC-ζ PS, such as with the db/db fibroblasts, protein expression of PKC-ζ, α-SMA, and RAGE is still downregulated suggesting that Rap1a plays a role in the AGE-RAGE signaling cascade shown in Figure 3.18, Figure 3.20, and Figure 3.21. Thus, these studies demonstrated AGE-RAGE signaling cascade can be downregulated by interrupting Rap1a GTPase crosstalk. PKC-ζ represents a key signaling hub linking the PKA and AGE-RAGE signaling cascade.

After analyzing the data, it became clear that another group of fibroblasts were needed to provide a complete picture for my project: AGE treated Het and db/db fibroblasts with ISO, EPAC Ag, or Rap1a siRNA. These cells would provide a better indication of the level of protein expression with ISO and EPAC Ag treatment compared to the PKC-ζ PS and AGE treatments. The data provided within this study suggests that activation of Rap1a stimulates downstream targets. These results are observed most effectively in db/db fibroblasts. Additional AGE treated cells combined with ISO or EPAC Ag treatments should simulate activation of downstream targets in Het samples similar to that of the db/db model.

Our data also demonstrates that protein expression in Het samples is near that of the universal control. A possible explanation, which is only speculation as of now, as to the lack of response in Het sample is that the AGE-RAGE cascade is uncoupled or not responsive, whereas the diabetic cells have an AGE-RAGE signaling cascade that is primed and responsive. Therefore, downstream targets like PKC-ζ, and ERK1/2, α-SMA, and RAGE are upregulated.

Collagen protein expression data was unable to be used since the data did not give a good representative of what was going on outside the fibroblasts. Collagen protein expression would have been proposed to be increased in ISO and EPAC Ag treated fibroblasts and those fibroblasts without the PS and PS + AGE treatments but decreased with Rap1a siRNA treated fibroblasts.

Collectively, the data provided potentially demonstrates that stimulation of Rap1a, either directly by EPAC Ag or indirectly by ISO, significantly increased phosphorylation levels of downstream AGE-RAGE signaling effectors, such as phospho-PKC-ζ and phospho-ERK1/2 in diabetic cardiac fibroblasts. Additionally, elevated phosphorylation levels of these proteins translated to significantly increased protein expression of known AGE-RAGE signaling outcomes, such as α-SMA and RAGE. Previous studies by our laboratory and others have demonstrated that upon activation of the AGE-RAGE signaling cascade multiple downstream signaling events can occur[8,30,33,35,74]. Downstream signaling events of AGE-RAGE cascade lead into three known outcomes: increased fibroblast differentiation marked by α-SMA protein levels, elevated RAGE protein expression, and increased collagen production. Isolated diabetic (db/db) cardiac fibroblasts had significantly greater levels of AGE-RAGE signaling

component activation and increased cascade outcomes in comparison to untreated non-diabetic (Het) fibroblasts. These data potentially demonstrate a positive correlation exists between Rap1a stimulation and increased AGE-RAGE cascade activation. However, further studies will need to be performed in order to confirm changes in collagen production. These findings are the first of its kind to provide Rap1a as a potential unique target for therapeutic strategies aimed at reducing chronic hyperglycemia-mediated ECM production and accumulation as well as fibroblast differentiation in the diabetic heart.

CHAPTER V

FUTURE DIRECTIONS

AGE treated fibroblast cells with Isoproterenol, EPAC Agonist, and Rap1a siRNA

After analyzing the data, we realized another group of fibroblasts was needed to provide a complete story. Het and db/db fibroblasts treated with AGE and one of the following: ISO, EPAC Ag, or Rap1a siRNA. Data from these fibroblast samples would confirm that changes in the protein expression levels as compared to untreated controls, PS treatments, and AGE + PS treatments. In addition, it would confirm that changes in protein expression levels of the PS vs. AGE + PS treatments were, in fact, due to the PS treatment. The data provided suggests that Rap1a activates downstream targets in db/db fibroblasts; however, having additional AGE treated fibroblasts along with ISO or EPAC Ag treatments should activate downstream target just like that of the db/db model. This would help support my hypothesis that Rap1a-dependent AGE/RAGE signaling occurs at PKC-ζ.

Collagen protein expression analysis

Unfortunately, the western blot membranes for collagen had a high degree of non-specific binding and was inconsistent across groups. Thus, not providing a clear picture of the signaling outcomes. More sensitive biochemical assays will need to be used to test for collagen expression levels. This knowledge could provide a better understanding of how Rap1a is interconnected with collagen production and fibrosis.

REFERENCES

1. Agrawal, N., Dasaradhi, P., Mohmmed, A., Malhotra, P., Bhatnagar, R., & Mukherjee, S. (2003). RNA Interference: Biology, Mechanism, and Applications. *Microbiology and Molecular Biology Reviews*; 67(4), 657–685.

2. Ahmed, M., Pelletier, J., Leumann, H., Gu, H., & Östenson, C. (2015). Expression of Protein Kinase C Isoforms in Pancreatic Islets and Liver of Male Goto-Kakizaki Rats, a Model of Type 2 Diabetes. *Plos ONE;* 10(9), 1-15.

3. American Diabetes Association. http://www.diabetes.org/diabetes-basics/?loc=GlobalNavDB

4. Arasteh, A., Farahi, S., Habibi-Rezaei, M., Moosavi-Movahedi, A. (2014). Glycated albumin: an overview of the *In Vitro* models of an *In Vivo* potential disease marker. *Journal of Diabetes & Metabolic Disorders;* 13, 49

5. Arthur, W., Quilliam, L., & Cooper, J. (2004). Rap1 Promotes Cell Spreading by Localizing Rac Guanine Nucleotide Exchange Factors. *The Journal of Cell Biology;* 167(1), 111.

6. Baum, J., & Duffy, H. (2011). Fibroblasts and myofibroblasts: what are we talking about? *Journal Of Cardiovascular Pharmacology;* 57(4), 376-379.

7. Banerjee, I., Fuseler J., Price R., et al. (2007). Determination of cell types and numbers during cardiac development in the neonatal and adult rat and mouse. *American Journal Of Physiology. Heart Circulatory Physiology;* 293(3), H1883-1891.

8. Bierhaus A., Humpert P., Morcos M., Wendt T., Chavakis T., et al. (2005). Understanding RAGE, the receptor for advanced glycation end products. *Journal Of Molecular Medicine (Berlin, Germany);* 83(11), 876-886.

9. Bogershausen, N., Tsai, I., Pohl, E., et al. (2015). Rap1-mediated mek/erk pathway defects in kabuki syndrome. *The Journal Of Clinical Investigation;* 125(9), 3585-3599.

10. Borg, T., Rubin, K., Lundgren, E., Borg, K., Obrink, B. (1984) Recognition of extracellular matrix components by neonatal and cardiac myocytes. *Developmental Biology;* 104(1), 86-96.

11. Bowers, S., et al. (2010). The extracellular matrix: at the center of it all. *Journal of Molecular and Cellular Cardiology;* 48(3), 474-482.

12. Burgess M., Carver, W., Terracio, L., et al. (1994). Integrin-mediated collagen gel contraction by cardiac fibroblasts: Effects of angiotensin II. *Circulation Research;* 74(2), 291-298.

13. Burgess M., Terracio L., Hirozane T., Borg T., (2002). Differential integrin expression by cardiac fibroblasts from hypertensive and exercise-trained rat hearts. *Cardiovascular Pathology;* 11(2), 78-87.

14. Busing K., Schulte-Sasse C., Fluchter S., Suselbeck T., Haase K., et al. (2005). Cerebral infarction: incidence and risk factors after diagnostic and interventional cardiac catheterization--prospective evaluation at diffusion-weighted MR imaging. *Radiology;* 235(1), 177-183.

15. Centers for Disease Control and Prevention. (2014). National Diabetes Statistics Report: Estimates of Diabetes and Its Burden in the United States, 2014. Atlanta, GA: US Department of Health and Human Services. http://www.cdc.gov/diabetes/data/statistics/2014statisticsreport.html

16. Chen-Izu, Y., Xiao, R., Izu, L., Cheng, H., Kuschel, M., Spurgeon, H., Lakatta, E. (2000). G_i-Dependent Localization of β_2-Adrenergic Receptor Signaling to L-Type Ca^{2+} Channels. *Biophysical Journal*. 79(5), 2547–2556.

17. de Rooij, J., Rehmann, H., van Triest, M., Cool, R., Wittinghofer, A., & Bos, J. (2000). Mechanism of regulation of the Epac family of cAMP-dependent RapGEFs. *Journal of Biological Chemistry;* 275(27), 20829-20836.

18. Dorsam, R., Gutkind, J. (2007). G-protein-coupled receptors and cancer. *Nature Reviews Cancer;* 7(2), 79–94.

19. Dudley, N. & Goldstein, B*. (2003). RNA interference: Silencing in the cytoplasm and nucleus. *Current Opinion in Molecular Therapeutics;* 5(2), 113-117.

20. Ehrhardt, A., Ehrhardt, G., Guo, X., Schrader, J. (2002). Ras and relatives--job sharing and networking keep an old family together. *Experimental Hematology;* 30(10), 1089-1106.

21. Faouzi, S., et al. (1999). Myofibroblasts are responsible for collagen synthesis in the stroma of human hepatocellular carcinoma: an *in vivo* and *in vitro* study. *Journal of Hepatology;* 30(2), 275-284.

22. Francis, S., & Corbin, J. (2004). Cyclic Nucleotide-Dependent Protein Kinases. *Encyclopedia of Biological Chemistry;* 1, 506-511.

23. Fritz, G. (2011). RAGE: A single receptor fits multiple ligands. *Trends in Biochemical Sciences;* 36(12), 625-632.

24. Gabbiani, G. (2003). The myofibroblast in wound healing and fibrocontractive diseases. *The Journal Of Pathology;* 200(4), 500-503.

25. Gordon, M. & Hahn, R. (2010). Collagens. *Cell And Tissue Research;* 339(1), 247-257.

26. Graham, H., Horn, M., & Trafford, A. (2008). Extracellular matrix profiles in the progression to heart failure. *Acta Physiologica;* 194(1), 3-21.

27. Haak, A., et al. (2014). Targeting the Myofibroblast Genetic Switch: Inhibitors of Myocardin-Related Transcription Factor/Serum Response Factor-Regulated Gene Transcription Prevent Fibrosis in a Murine Model of Skin Injury. *The Journal Of Pharmacology and Experimental Therapeutics;* 349(3), 480-486.

28. Hamilton A., Baulcombe, D. (1999). A species of small antisense RNA in posttranscriptional gene silencing in plants. *Science;* 286(5441), 950–952.

29. Hammond, S., Bernstein, E., Beach, D., & Hannon, G. (2000). An RNA-directed nuclease mediates post-transcriptional gene silencing in *Drosophila* cells. *Nature;* 404(6775), 293–296.

30. Haslbeck K., Schleicher E., Bierhaus A., Nawroth P., Haslbeck M., et al. (2005). The AGE/RAGE/NF-(kappa)B pathway may contribute to the pathogenesis of polyneuropathy in impaired glucose tolerance (IGT). *Experimental And Clinical Endocrinology & Diabetes: Official Journal, German Society Of Endocrinology [And] German Diabetes Association;* 113(5), 288-291.

31. Hegab, Z., et al. (2012). Role of advanced glycation end products in cardiovascular disease. *World Journal Of Cardiology;* 4(4), 90-102.

32. Heidland, A., Sebekova, K., Schinzel, R. (2001). Advanced glycation end products and the progressive course of renal disease. *American Journal Of Kidney Diseases: The Official Journal Of The National Kidney Foundation;* 38(4 Suppl 1), S100-6.

33. Hofmann, M., Drury, S., Fu, C., Qu, W., Taguchi, A., et al. (1999). RAGE mediates a novel proinflammatory axis: a central cell surface receptor for S100/calgranulin polypeptides. *Cell;* 97(7), 889-901.

34. Hurowitz, E., Melnyk, J., Chen, Y., Kouros-Mehr, H., Simon, M., Shizuya, H. (2000). Genomic characterization of the human heterotrimeric G-protein alpha, beta, and gamma subunit genes. *DNA Research: An International Journal For Rapid Publication Of Reports On Genes And Genomes;* 7(2), 111–120.

35. Hutchinson, K., Lord, C., et al. (2013). Cardiac fibroblast-dependent extracellular matrix accumulation is associated with diastolic stiffness in type 2 diabetes. *PLoS One;* 8(8), e72080.

36. Insel, P., Murray, F., et al. (2012). cAMP and Epac in the regulation of tissue fibrosis. *British Journal Of Pharmacology;* 166(2), 447-456.

37. Jeyaraj, S., Unger, N., et al. (2011). Rap1 GTPases: an emerging role in the cardiovasculature. *Life Sciences;* 88(15-16), 645-652.

38. Katz, S., Boland, R., Santillan, G. (2006). Modulation of ERK 1/2 and p38 MAPK signaling pathways by ATP in osteoblasts: involvement of mechanical stress-activated calcium influx, PKC and Src activation. *International Journal Of Biochemistry And Cell Biology;* 38(12), 2082-2091.

39. Kang, G., et al. (2003). Epac-selective cAMP Analog 8-pCPT-2'-*O*-Me-cAMP as a Stimulus for Ca^{2+}-induced Ca^{2+} Release and Exocytosis in Pancreatic β-Cells*. *Journal Of Biological Chemistry;* 278(10), 8279-8285.

40. Kekalainen, K., et al. (1999). Hyperinsulinemia Cluster Predicts the Development of Type 2 Diabetes Independently of Family History of Diabetes. *Diabetes Care;* 22(1), 86-92.

41. Khoshnoodi, J., Pedchenko, V., Hudson, B., (2008). Mammalian Collagen IV. *Microscopy Research And Technique;* 71(5), 357-370.

42. Koch, M., Chitayat, S., et al. (2010). Structural basis for ligand recognition and activation of RAGE. *Structure;* 18(10), 1342-1352.

43. Koya, D., Haneda, M., Nakagawa, H., Isshiki, K., Sato, H., Maeda, S., Sugimoto, T., Yasuda, H., Kashiwagi, A., Ways, D, King, G., & Kikkawa, R. (2000). Amelioration of accelerated diabetic mesangial expansion by treatment with a PKC beta inhibitor in diabetic db/db mice, a rodent model for type 2 diabetes. *FASEB Journal: Official Publication Of The Federation Of American Societies For Experimental Biology;* 14(3), 439-447.

44. May, L., & Hill, S. (2008). ERK phosphorylation: Spatial and temporal regulation by G-protein-coupled receptors. *The International Journal of Biochemistry & Cell Biology;* 40(10), 2013-2017.

45. Metz, V., et al. (2012). Induction of RAGE shedding by activation of G-protein-coupled receptors. *PLoS One;* 7(7), e41823.

46. Münch, G., Schicktanz, D., Behme, A., Manfred Gerlach, M., Riederer, P., Palm, R., & Schinzel, R. Amino acid specificity of glycation and protein-AGE crosslinking reactivities determined with a dipeptide SPOT library. *Nature Biotechnology;* 17(10), 1006-1010.

47. National Diabetes Information Clearinghouse. (2014). Causes of Diabetes. National Institutes of Health. Pub No. 14-5164. www.diabetes.niddk.nih.gov

48. National Diabetes Information Clearinghouse. (2013). Your Guide to Diabetes: Type 1 and Type 2. National Institutes of Health. Pub No. 14–4016. www.diabetes.niddk.nih.gov

49. Orgel, J., Irving, T., Miller, A., Wess, T. 2006. Microfibrillar structure of type I collagen *in situ*. *Proceedings of the National Academy of Sciences of the United States of America;* 103(24), 9001–9005.

50. Peacock, J., Lu, Y., Koch, M., Kadler, K., Lincoln, J. (2008). Temporal and spatial expression of collagens during murine atrioventricular heart valve development and maintenance. *Developmental Dynamics: An Official Publication Of The American Association Of Anatomists;* 237(10), 3051-3058.

51. Penfold, S., Coughlan, M., Patel, S., Srivastava, P., Sourris, K., Steer, D., Webster, D., Thomas, M., MacIsaac, R., Jerums, G., Burrell, L., Cooper, M., Forbes, J. (2010). Circulating high-molecular-weight RAGE ligands activate pathways implicated in the development of diabetic nephropathy. *Kidney International;* 78(3), 287-295.

52. Ramasamy, R., et al. (2005). Advanced glycation end products and RAGE: a common thread in aging, diabetes, neurodegeneration, and inflammation. *Glycobiology;* 15(7), 16R-28R.

53. Ramasamy, R., Yan, S., et al. (2011). Receptor for AGE (RAGE): signaling mechanisms in the pathogenesis of diabetes and its complications. *Annals of the New York Academy of Sciences;* 1243(1), 88-102.

54. Ramos, J., (2008). The regulation of extracellular signal-regulated kinase (ERK) in mammalian cells. *The International Journal of Biochemistry & Cell Biology;* 40(12), 2707-2719.

55. Ramos, K., & Weber, T. (2010). 2.23: Introduction and Overview of Alterations in Cell Signaling. *Comprehensive Toxicology;* 447-471.

56. Ricard-Blum, S. (2011). The Collagen Family. *Cold Spring Harbor Perspectives In Biology;* 3(1), a004978.

57. Ricard-Blum, S. & Ruggiero, F. (2005). The collagen superfamily: from the extracellular matrix to the cell membrane. *Pathologie Biologie* (Paris*);* 53(7), 430-442.

58. Sakaguchi, M., Murata, H., Yamamoto, K., Ono, T., Sakaguchi, Y., Motoyama, A., Hibino, T., Kataoka, K., & Huh, N. (2011). TIRAP, an Adaptor Protein for TLR2/4, Transduces a Signal from RAGE Phosphorylated upon Ligand Binding. *Plos ONE;* 6(8), 1-10.

59. Santa Cruz Biotechnology. (2015). http://www.scbt.com/datasheet-3098-pkc-zeta-pseudo-substrate-inhibitor.html

60. Santoni, G., Cardinali, C., Morelli, M. B., Santoni, M., Nabissi, M., & Amantini, C. (2015). Danger- and pathogen-associated molecular patterns recognition by pattern-recognition receptors and ion channels of the transient receptor potential family triggers the inflammasome activation in immune cells and sensory neurons. *Journal of Neuroinflammation;* 12(1), 1-10.

61. Schmidt A., Yan S., Wautier J., et al. (1999). Activation of receptor for advanced glycation end products: A mechanism for chronic vascular dysfunction in diabetic vasculopathy and atherosclerosis. *Circulation Research;* 84(5), 489-497.

62. Shaul, Y., & Seger, R. (2007). Review: The MEK/ERK cascade: From signaling specificity to diverse functions. *BBA - Molecular Cell Research;* 1773(8), 1213-1226.

63. Soman, S., Raju, R., Sandhya, V., Advani, J., Khan, A., Harsha, H., Prasad, T., Sudhakaran, P., Pandey, A., and Adishesha, P. (2013). A multicellular signaling transduction network of AGE/RAGE signaling. *Journal Of Cell Communication And Signaling;* 7(1), 19-23.

64. Souders, C., et al. (2009). Cardiac fibroblast: the renaissance cell. *Circulation Research;* 105(12), 1164-1176.

65. Stewart J., Jr., Cashatt D., Borck A., et al. (2006). 17beta-estradiol modulation of angiotensin ii-stimulated response in cardiac fibroblasts. *Journal Of Molecular And Cellular Cardiology;* 41(1), 97-107.

66. Subramanian, J., Dye, L., Morozov, A. (2013) Rap1 signaling prevents l-type calcium channel-dependent neurotransmitter release. *The Journal of Neuroscience: The Official Journal Of The Society For Neuroscience;* 33(17), 7245-7252.

67. Takahra, T., Smart, D., Oakley, F., & Mann, D. (2004). Induction of myofibroblast MMP-9 transcription in three-dimensional collagen I gel cultures: regulation by NF-κB, AP-1, and Sp1. *International Journal of Biochemistry And Cell Biology;* 36(2), 353–363.

68. Tomasek, J., Gabbiani, G., Hinz, B., Chaponnier, C., & Brown, R. (2002). Myofibroblasts and mechano-regulation of connective tissue remodelling. *Nature Reviews. Molecular Cell Biology;* 3(5), 349-363.

69. van Dijk, F., Huizer, M., Kariminejad, A., Marcelis, C., Plomp, A., Terhal, P., Meijers-Heijboer, H., Weiss, M., van Rijn, R, Cobben, J., Pals, G. (2010). Complete COL1A1 allele deletions in osteogenesis imperfecta. *Genetics In Medicine: Official Journal Of The American College Of Medical Genetics;* 12(11), 736-741.

70. Watson, James D. (2008). Molecular Biology of the Gene. San Francisco, CA: Cold Spring Harbor Laboratory Press; 7th Ed., 711–730.

71. Weber, K., Pick, R., Jalil, J., Janicki, J. & Carroll, E. (1989). Patterns of myocardial fibrosis. *Journal Of Molecular And Cellular Cardiology;* 21(Suppl 5),121-131.

72. Weber, T. (2010). 2.24: Protein Kinases. *Comprehensive Toxicology;* 473-493.

73. Weis, M., et al. (2010). Location of 3-Hydroxyproline Residues in Collagen Types I, II, III, and V/XI Implies a Role in Fibril Supramolecular Assembly. *The Journal Of Biological Chemistry;* 285(4), 2580-2590.

74. Wendt, T., Tanji, N., Guo, J., Hudson, B., Bierhaus, A., et al. (2003). Glucose, glycation, and RAGE: implications for amplification of cellular dysfunction in diabetic nephropathy. *Journal Of The American Society Of Nephrology;* 14(5), 1383-1395.

75. Wynn, T., & Ramalingam, T. (2012). Mechanisms of fibrosis: therapeutic translation for fibrotic disease. *Nature Medicine;* 18(7), 1028–1040.

76. Xu, A., Butler, A., & Barsh, G., (2008). Rodent Models of Obesity: Natural Monogenic Models. Obesity: Genomics and Postgenomics. Informa Healthcare; 3.1: 77-87.

77. Yan, S., Ramasamy, R., Naka, Y., et al. (2003). Glycation, inflammation, and rage: A scaffold for the macrovascular complications of diabetes and beyond. *Circulation Research;* 93(12), 1159-1169.

78. Yang, R., & Barouch, L., (2007). Leptin Signaling and Obesity: Cardiovascular Consequences. *Circulation Research;* 101(6), 545-559.

79. Yu, L., Zhao, Y., Xu, S., Ding, F., Jin, C., et al. (2013). Advanced Glycation End Product (AGE)-AGE Receptor (RAGE) System Upregulated Connexin43 Expression in Rat Cardiomyocytes via PKC and Erk MAPK Pathways. *International Journal of Molecular Sciences;* 14(2), 2242-2257.

80. Yuen, A., Laschinger, C., Talior, I., et al. (2010). Methylglyoxal-modified collagen promotes myofibroblast differentiation. *Matrix Biology;* 29(6), 537-548.

81. Zehorai, E., Yao, Z., Plotnikov, A., Seger, R. (2010). Review: The subcellular localization of MEK and ERK--A novel nuclear translocation signal (NTS) paves a way to the nucleus. *Molecular and Cellular Endocrinology;* 314(2), 213-220.

82. Zhang, X., J. A. Stewart, Jr., et al. (2007). Effects of elevated glucose levels on interactions of cardiac fibroblasts with the extracellular matrix. *In Vitro Cellular & Developmental Biology. Animal;* 43(8-9), 297-305.

83. Zhao, J., Randive, R., Stewart, J. (2014). Molecular mechanisms of AGE/RAGE-mediated fibrosis in the diabetic heart. *World Journal Of Diabetes;* 5(6), 860-867

84. Zou, Y., Komuro, I., Yamazaki, T., et al. (1999). Both G_s and G_i Proteins Are Critically Involved in Isoproterenol-induced Cardiomyocyte Hypertrophy. *The Journal Of Biological Chemistry;* 274(14), 9760-9770.

85. The Jackson Laboratory. (2016) https://www.jax.org/strain/000642